

Reconnaissance geochemical mapping of the Maniitsoq region (65° to 66°N, 51°45' to 53°30'W), southern West Greenland

Agnete Steenfelt, Anette Petersen  
and Else Dam

Open File Series 94/5



February 1994



GRØNLANDS GEOLOGISKE UNDERSØGELSE  
Ujarassioortut Kalaallit Nunaanni Misissuisoqarfiat  
GEOLOGICAL SURVEY OF GREENLAND

**GRØNLANDS GEOLOGISKE UNDERSØGELSE**  
**Ujarassiortut Kalaallit Nunaanni Misissuisoqarfiat**  
**GEOLOGICAL SURVEY OF GREENLAND**

Øster Voldgade 10, DK-1350 Copenhagen K, Denmark

The Geological Survey of Greenland (GGU) is a research institute affiliated to the Mineral Resources Administration for Greenland (MRA) within the Danish Ministry of Energy. As with all other activities involving mineral resources in Greenland, GGU's investigations are carried out within the framework of the policies decided jointly by the Greenland Home Rule Authority and the Danish State.

**Open File Series**

The Open File Series consists of unedited reports and maps that are made available quickly in limited numbers to the public. They are a non-permanent form of publication that may be cited as sources of information. Certain reports may be replaced later by edited versions.

**Citation form**

*Open File Series Grønlands Geologiske Undersøgelse*

conveniently abbreviated to:

*Open File Ser. Grønlands geol. Unders.*

GGU's Open File Series består af uredigerede rapporter og kort, som publiceres hurtigt og i et begrænset antal. Disse publikationer er midlertidige og kan anvendes som kildemateriale. Visse af rapporterne vil evt. senere blive erstattet af redigerede udgaver.

ISSN 0903-7322

**GRØNLANDS GEOLOGISKE UNDERSØGELSE**

**Open File Series 94/5**

**Reconnaissance geochemical mapping of the Maniitsoq region  
(65° to 66°N, 51°45' to 53°30'W), southern West Greenland**

**Agnete Steenfelt, Anette Petersen and Else Dam**

**February 1994**

## **Abstract**

Geochemical mapping by means of analysis of stream sediment and water collected at a density of 1 sample per 20-30 km<sup>2</sup> has been carried out over part of the Archaean craton in the Maniitsoq region of West Greenland. The <0.1 mm fraction of the sediment samples was analysed by X-ray fluorescence and instrumental neutron activation techniques and results are reported for 41 major and trace elements. The conductivity and fluoride contents of the water samples were also determined.

The distribution of geochemical anomalies in the survey area indicates possibilities for: (1) gold mineralisation associated with noritic intrusions and shear zones; (2) chromium-nickel mineralisation in dunitic rocks. One anomaly indicates a new occurrence of carbonatite or a related rock type.

**Contents**

Introduction . . . . .	4
Geology . . . . .	4
Mineral exploration . . . . .	5
Physiography . . . . .	6
Sampling . . . . .	6
Sample preparation and analysis . . . . .	7
Data presentation . . . . .	7
Comments on the element distribution patterns . . . . .	8
Element distribution indicating mineralisation . . . . .	9
Conclusion . . . . .	11
Acknowledgements . . . . .	11
References . . . . .	11
Table 1, 2 & 3 . . . . .	14
List of figures . . . . .	15

## Introduction

The sampling carried out in the Maniitsoq region is part of the Geological Survey of Greenland (GGU) geochemical mapping programme based on drainage samples. The purpose of this programme is to provide reconnaissance geochemical data which may be used together with geophysical and geological information to outline provinces or zones with potential for mineral resources.

Samples were collected during the period August 5th to 11th by A. Petersen and C. Z. Munch-Andersen. The sampling team was based at Maniitsoq (Sukkertoppen) and used an AS 350 (Ecureuil) helicopter for transportation. The field and analytical work was financially supported by the Mineral Resource Administration for Greenland, part of the Danish Ministry of Energy.

The surveyed area lies administratively within the municipality of Maniitsoq (Sukkertoppen).

## Geology

The Maniitsoq region is situated in the northern part of the Archaean gneiss complex of West Greenland. A geological map of the region at the scale of 1:500 000 (Allaart, 1982) covers the region. The publications by Kalsbeek & Garde (1989) and Bridgwater *et al.* (1976) contain summary descriptions of the area and comprehensive literature references.

The north-western part of the surveyed area consists of Archaean granulite facies orthogneisses of tonalitic to granodioritic composition (enderbite) which contain layers and enclaves of supracrustal sequences. The south-eastern part mainly comprises amphibolite facies rocks: grey foliated biotite and hornblende gneiss and the tonalitic Finnefjeld complex interpreted to be a tonalitic intrusive complex into the gneisses (Marker & Garde, 1988). Granulite facies gneisses only occur on both sides of Søndre Isortoq (Fig. 1). The supracrustal units intercalated with the gneisses over the entire area comprise both basic metavolcanics (amphibolites) and metasediments.

The south-eastern part of the Maniitsoq region is believed to belong to the Akia terrane defined by Friend *et al.* (1988). This terrane was subjected to granulite facies metamorphism at about 3000 Ma. An age estimate for the Finnefjeld complex also gives

c. 3000 Ma (Garde, 1990). In contrast, isotopic data from Hamborgerland (Kalsbeek, 1993; Friend and Nutman, in press) indicate that the deposition of sediments and subsequent granulite facies metamorphism in that area took place later, around 2700 Ma. It would seem, therefore, that a terrane boundary is located between the Finnefjeld complex and Hamborgerland. The geology of the Akia terrane has mainly been studied outside the present survey area (Garde, 1990; McGregor *et al.*, 1991).

A number of small norite bodies of assumed late Archaean age (Kalsbeek & Garde, 1989) have intruded the gneisses and Finnefjeld complex. A few are found inside the survey area while the majority occur in an elongate belt east of the area.

The prominent Evighedsfjord shear zone (ESZ) of assumed Archaean age transects the north-western part of the region (Fig. 1). The granulite facies gneisses have been retrogressed to amphibolite facies along the shear zone. Minor shear zones east of ESZ are parallel to it, while shear zones with an ENE trend transect the Finnefjeld complex and the surrounding gneisses. The age relations between the various sets of shears have not been worked out but it is probable that the shear zones were active during Proterozoic time and later (Knudsen, 1991).

A major doleritic dyke swarm of Proterozoic age intruded into the north-western part of the region (Windley, 1970). The dykes are known as Kangamiut dykes and they are assumed to be related to the evolution of the Proterozoic Nagssugtoqidian mobile belt north of the survey area.

The Maniitsoq region lies within a province of recurrent alkaline magmatism described in Larsen (1991) and Larsen & Rex (1992). The small Archaean (2656 Ma) Tupertalik carbonatite (Larsen & Pedersen, 1982) and late Proterozoic (c. 600 Ma) kimberlites are within the present map area. The Mesozoic (175 Ma) Qaqarssuk carbonatite complex with associated monchiquitic dykes (Knudsen, 1991) lies immediately to the east of the surveyed area.

### **Mineral exploration**

Most mineral exploration activities have been carried out by Kryolitselskabet Øresund A/S (KØ) (1973; Appel & Lind, 1990) and their main target was Pt bearing Cu-Ni sulphide mineralisation associated with the suite of noritic intrusions (see also Secher, 1983). Two of the prospects investigated are situated within the survey area while the

majority are east of the survey border. In one (Qerrulik, see Fig. 44) disseminated to massive sulphide mineralisation was estimated by surface sampling and drilling to contain 0.5 mill t of ore with 0.06 % Cu and 0.13 % Ni. The other occurrence of disseminated sulphide mineralisation (Pingo, see Fig. 44) is hosted by a 4 km long and less than 100 m wide tectonised norite body and has yielded concentrations in the order of 0.2-0.3 % Cu and 0.3-0.6 % Ni. Localities with PGE and Au contents of the sulphide mineralisation hosted by norites are shown in Appel & Lind (1990).

### **Physiography**

The surveyed area is mountainous with peaks commonly rising to more than 600 m in the coastal areas, and to more than 1500 m at the inner part of Evighedsfjord and around the edge of the large ice cap in the western part of the region. Outside the ice caps the distribution of streams is sufficiently even to allow systematic sampling. A number of samples were collected at the front of glacier tongues radiating from local ice caps. Present day erosion of the crystalline rocks is weak, except in the glaciated areas, and fine material is scarce in many streams. As a result, a number of the samples did not contain enough fine fraction material for the entire analytical programme. The bedrock exposure is exceptionally good in this region.

### **Sampling**

Eight working days and 26.5 helicopter flying-hours were spent during the sampling of 215 sites distributed over 5600 km<sup>2</sup> (exclusive of ice caps). On average 28 samples were collected per day at an average density of 1 site per 26 km<sup>2</sup>; 7 flying minutes were spent per sampling site, which corresponds to 17 flying seconds per km<sup>2</sup>.

The sample sites were selected and marked on aerial photographs prior to the sampling, using criteria such as even distribution of the sites, a reasonable size of upstream drainage area, and a reasonable slope dip.

At each station *c.* 500 g of stream sediment was collected in a paper bag and 100 ml of stream water in a polyethylene bottle. In addition the radioactivity (total gamma-radiation) was measured on the surface of outcrops or stream boulders using a scintillometer (Table 1). To increase the representivity, each stream sediment sample was composed of

subsamples from 3 to 7 different sites of sand and silt deposits in the stream bed or banks. Duplicate samples of both sediment and water were collected at 9 localities, which corresponds to 4 % of the total number of sample localities.

In addition to the sampling for the reconnaissance geochemical mapping a measurement of the gravity field was made at each locality by E. Hansen, who joined the geochemistry sampling team. The methodology and results of the gravity survey will be reported separately in the GGU Open File Series.

### **Sample preparation and analysis**

Sediment. The sample bags were dried at room temperature at the base-camp in Maniitsoq and then sent by ship to GGU, Copenhagen. Here the samples were further dried at 65°C and sieved into three grain size fractions using sieve apertures of 1 mm and 0.1 mm. The coarse fraction was discarded, the medium fraction archived, and the fine fraction submitted for analysis. The samples were analysed by the instrumental neutron activation (INA) method for Au and 34 other elements and by X-ray fluorescence spectrometry using pressed powder tablets for 14 trace elements (XRF-trace) at Activation Laboratories Ltd, Canada. They were analysed for major elements at the Geological Survey of Greenland by X-ray fluorescence spectrometry on fused discs, using Na-tetraborate, except Na<sub>2</sub>O which was determined by atomic absorption spectrophotometry together with Cu. Some samples did not contain sufficient amounts of fine fraction to permit all three types of analysis, and this explains the different numbers of samples analysed: 211 INA, 173 XRF-trace, and 185 XRF-major.

Water. The water samples (totalling 222) were sent by ship to GGU, Copenhagen, where they were analysed c. 2 months after collection. The conductivity and fluoride concentrations were measured (Table 1).

### **Data presentation**

The analytical results from the Maniitsoq region are shown in this report as element distribution maps at 1:1 000 000 scale together with summary statistical parameters and histograms of the frequency distribution for each element (Figs 2 to 43).

Elements with insignificant concentrations, i.e. at or below the detection limit (Table 2), are not presented. In cases where an element has been determined by more than one method, only one of the data sets is presented: that regarded as the most reliable or determined at the lowest detection limit. The major elements are expressed as oxides and the plots represent analytical values recalculated as volatile free components. The amount of volatiles (as determined by loss on ignition) is on average 4.2 % (maximum value is 17.4 % and minimum 0 %). High amounts of volatiles were measured in samples with a high proportion of organic matter.

In the element distribution maps the size of a dot is proportional to the concentration in the sample. The scaling of the dot size is chosen so that regional variations in the geochemical background are displayed as clearly as possible. Maximum values are found in the statistical parameters in the figures, and values regarded as geochemical anomalies are shown on the anomaly map (Fig. 44).

### **Comments on the element distribution patterns**

In general the element distribution patterns reflect the litho-geochemical variation over the survey area and high values for some elements can often be interpreted to indicate mineralisation. In the Maniitsoq region the main contributors to the litho-geochemical variation are the gneisses, the supracrustal and infracrustal enclaves and granites/pegmatites.

The main geochemical features are: (1) higher concentrations of  $\text{TiO}_2$ ,  $\text{Fe}_2\text{O}_3$ ,  $\text{MnO}$ ,  $\text{CaO}$ ,  $\text{Ba}$ ,  $\text{Co}$ ,  $\text{Cu}$ ,  $\text{Sc}$  and  $\text{V}$  in the north-western part of the region than in the south-eastern; (2) a "corridor" with a north-east trend from Maniitsoq island and Hamburgerland to inner Evighedsfjord distinguished by high  $\text{K}_2\text{O}$ ,  $\text{Hf}$ ,  $\text{Rb}$ ,  $\text{Th}$ ,  $\text{La}$  and low  $\text{Sr}$ ; (3) Some high values of  $\text{MgO}$ ,  $\text{CaO}$ ,  $\text{Co}$ ,  $\text{Cr}$  and  $\text{Ni}$  along Søndre Isortoq in an area that otherwise has a low level of these elements.

The first feature agrees with the predominance of granulite facies rocks with enclaves and numerous dykes of basic composition NW of the Evighedsfjord shear zone (ESZ). Geologically and geochemically it is a continuation of the region to the north (Steenfelt *et al.*, 1993).

The "lithophile corridor" is not correlatable with any feature in the geological map. Minor occurrences of K-feldspar rich granites were observed in the inner Evighedsfjord

area during sampling, and granitic gneiss and pegmatites were observed locally east of the abandoned settlement Ikamiut. A white garnet bearing granitoid rock occurs at the north coast of Hamburgerland. The high Mg, Cr and Ni values along Søndre Isortoq indicate occurrences of ultramafic rocks as enclaves in the gneisses.

A single sample at a locality 65°30'N and 52°W has an anomalous composition with very high Fe<sub>2</sub>O<sub>3</sub>, MgO, CaO, Ba, Co, Cr, Cu, Eu and V (Table 3). The element association is typical for carbonatitic rocks which indicates that a small unknown complex like that at Tupertalik may occur in the drainage area. The large Qaqarsuk carbonatite complex (Knudsen, 1991) causes elevated Nb concentrations in samples from the main valley draining the complex.

The Finnefeld complex is low in lithophile elements which would point to a calc-alkaline affinity in agreement with its tonalitic composition.

The geochemical differences noted between the north-western and south-eastern parts of the region seem to support the ideas discussed by Kalsbeek (1993) and Friend & Nutman (in press) of the possible existence of an Archaean terrane boundary located in the Maniitsoq region.

### **Element distribution indicating mineralisation**

Figure 44 shows the distribution of the highest values for selected elements.

*Gold.* 39 samples had gold above the detection limit (5 ppb), and of these 6 were above 10 ppb. Their distribution does not point to any particularly favourable rock association or site. The pathfinder elements As and Sb also have low concentrations. However, it is worth noting (Fig. 13) that a cluster of slightly elevated Au values occur round the sulphide mineralised norite occurrence, Qerrulik (Q in Fig. 13), investigated by KØ. The highest value (15 ppb) in that cluster occurs downstream from the norite outcrop. Near the Pingo (P in Fig. 13) sulphide mineralised norite occurrence, gold is also slightly enriched. The highest gold value recorded in the present survey (61 ppb) lies on a topographical lineament which may represent a fault or a shear zone. It is possible that the distribution of the other gold containing samples reflects gold mineralisation associated with shear and fault zones.

*Nickel and chromium.* The highest Ni and Cr values are located at 3 sites. The southernmost is located in an area with known dunites. These have been registered by KØ

and were visited by the first author in 1981. A stream sediment sample draining an outcropping dunite was collected then and had a Cr concentration of about 0.1 % and Ni concentration of 654 ppm. The north-eastern anomaly is a combined Ni-Cr-Co anomaly. It is situated in a cluster of Cr-Ni-Co anomalies registered in the neighbouring area (Steenfelt *et al.*, 1990). The cluster surrounds the Pingo noritic body with disseminated to semimassive sulphide mineralisation (Kryolitselskabet Øresund A/S, 1973). During the first author's reconnaissance in 1981 another dunitic body was located on the south shore at Evighedsfjord (loc. A in Fig. 44). A stream sediment sample from the dunite gave *c.* 0.1 % Cr and 2665 ppm Ni.

*Base metals.* The highest values are located in the north-western area. Enclaves of supracrustal rocks often contain rusty zones reflecting sulphide mineralisation. However, it must be borne in mind that the Kangamiut dykes probably contain of the order of 100 ppm Cu and 100 ppm Zn, and a dyke occurring close to a sampling site may create elevated Cu and Zn concentrations.

*Uranium and thorium.* High concentrations of Th are located in the "lithophile corridor" and probably reflect the presence of radioactive pegmatites. By contrast, the highest U values are located in the south-western part where they form an elongated cluster. During the 1981 reconnaissance in that area uranium minerals were observed in pegmatites and in a shear zone. The anomaly pattern and the field observations suggest a structural control of the uranium mineralisation.

*Kimberlites.* The kimberlite dykes which have been located within the survey area are listed in Larsen (1991). The dykes are rarely more than 0.5 m wide and are not likely to be reflected in the stream sediment chemistry unless they outcrop close to a sampling site. The characteristic chemistry is high MgO, Ba, Sr, La, Nb, Cr, and Ni. This combination is not found. The closest is the composition of the multielement anomaly shown in Figure 44 which, however, is low in Nb, and could just as well be indicative of a carbonatite occurrence. On the other hand the unexpected high Nb concentration (30 ppm, Fig. 21) found at the peninsula south of Søndre Isortoq is combined with high La and could be indicative of kimberlite.

## Conclusion

The geochemical survey of the Maniitsoq region in the Archaean craton in West Greenland outlines some regional geochemical differences which may contribute to the understanding of relationships between crustal domains in the Archaean. A new occurrence of carbonatite or other alkaline magmatic rock is indicated on the north side of Søndre Isortoq.

The distribution patterns of ore forming elements combined with results of earlier work suggest that the most favourable targets for exploration are the norite intrusions (Au, PGE), shearzones (Au), the ultrabasic bodies (Cr, Ni), and kimberlites (diamonds).

## Acknowledgements

The authors are grateful to Christian Z. Munch-Andersen for sample collection and field assistance. The sampling benefitted greatly from the skill and enthusiastic cooperation of the UNIFLY helicopter pilot Hans Hammer.

## References

- Allaart, J. H. 1982: Geological Map of Greenland, 1:500 000, sheet 2, Frederikshåb Isblink to Søndre Strømfjord. Copenhagen: Grønlands Geologiske Undersøgelse.
- Appel, P. W. U. & Lind, M. 1990: Thematic maps 90/1-401 to 90/1-405 Mineral Occurrences. In Steenfelt, A., Thorning, L. & Tukiainen, T. (ed.) *Regional compilations of geoscience data from the Nuuk-Maniitsoq area, southern West Greenland*. Thematic Map. Ser. Grønlands geol. Unders. 90/1.
- Bridgwater, D., Keto, L. & McGregor, V. R. 1976: Archaean gneiss complex of Greenland. In Escher, A. & Watt, W. S. (ed.) *Geology of Greenland*, 18-75. Copenhagen: Grønlands Geologiske Undersøgelse.
- Friend, C. R. L., Nutman, A. P. & McGregor, V. R. 1988: Late Archaean terrane accretion in the Godthåb region, southern West Greenland. *Nature* 335, 535-538.
- Friend, C. R. L. & Nutman, A. P. in press: Two Archaean granulite facies metamorphic events in the Nuuk-Maniitsoq region, West Greenland: correlation with the Sagleg block, Labrador. London: J. geol. Soc.

- Garde, A. A. 1990: Thermal granulite-facies metamorphism with diffuse retrogression in Archaean orthogneisses, Fiskefjord, southern West Greenland. *J. metamorphic Geol.* **8**, 663-682.
- Kalsbeek, F. 1993: Use of Rb-Sr isotope data to constrain the time of deposition of Precambrian metasediments: an example from Hamborgerland, West Greenland. *Rapp. Grønlands geol. Unders.* **159**, 95-100.
- Kalsbeek, F. & Garde, A. A. 1989: Descriptive text to 1:500 000 sheet 2, Frederikshåb Isblink to Søndre Strømfjord, 36 pp. Copenhagen: Grønlands Geologiske Undersøgelse.
- Knudsen, C. 1991: Petrology, geochemistry and economic geology of the Qaqarssuk carbonatite complex, southern West Greenland. Monograph Series on Mineral Deposits 29, 1-110. Berlin: Gebrüder Borntraeger.
- Juhava, R., Keto, L., Kurki, J. & Turkka, S. 1973: Report on selected sulphide mineralizations in noritic rocks. Compilation of KØ-reports 1965-1972. Internal report, Kryolitselskabet Øresund A/S, 182 pp. (GREENMIN ref. no. 1276).
- Larsen, L. M. 1991: Occurrences of kimberlite, lamproite and ultramafic lamprophyre in Greenland. *Open File Ser. Grønlands geol. Unders.* **91/2**, 36 pp.
- Larsen, L. M. & Pedersen, A. K. 1982: A minor carbonatite occurrence in southern West Greenland: the Tupertalik intrusion. *Rapp. Grønlands geol. Unders.* **110**, 38-43.
- Larsen, L. M. & Rex, D. 1992: A review of the 2500 Ma span of alkaline-ultramafic, potassic and carbonatitic magmatism in West Greenland. *Lithos* **28**, 367-402.
- Marker, M. & Garde, A. A. Border relations between the amphibolite Finnefjeld gneiss complex and granulite facies grey gneisses in the Fiskefjord area, southern West Greenland. *Rapp. Grønlands geol. Unders.* **140**, 49-54.
- McGregor, V. R., Friend, C. R. L. & Nutman, A. P. 1991: The late Archaean mobile belt through Godthåbsfjord, southern West Greenland: a continent-continent collision zone? *Bull. geol. Soc. Denmark* **39**, 179-197.
- Secher, K. 1983: Noritic rocks and associated nickel-copper-sulphide occurrences in Sukkertoppen district, central West Greenland. *Rapp. Grønlands geol. Unders.* **115**, 30-34.
- Steenfelt, A., Nielsen, J. P. & Dam, E. 1993: Reconnaissance geochemical mapping of map sheets 67 V.1 and 68 V.1 (66° to 68°N, 51°40' to 54°W), West Greenland. *Open File Ser. Grønlands geol. Unders.* **93/1**, 16 pp.

Windley, B. F. 1970: Primary quartz ferro-dolerite/garnet amphibolite dykes in the Sukkertoppen region of West Greenland. *In* Newall, G. & Rast, N. (ed.) *Mechanics of igneous intrusions*, 79-92. Liverpool: Gallery Press.

Table 1. Instrumentation at the Geological Survey of Greenland

Field measurement of gamma-radiation: Saphymo-Srat SPP-2 scintillometer

Water samples:

Conductivity: Chemotest JK 8800

Fluoride concentration: Orion EA 920 pH/ion analyzer

Table 2. Analytical detection limits

Instrumental Neutron Activation Analysis (Activation Laboratories Ltd.)

Au	5.0	ppm	Ag	5.0	ppm	As	2.0	ppm	Ba	100.0	ppm
Br	1.0	ppm	Ca	1.0	%	Co	5.0	ppm	Cr	10.0	ppm
Cs	2.0	ppm	Fe	0.02	%	Hf	1.0	ppm	Hg	1.0	ppm
Ir	5.0	ppm	Mo	5.0	ppm	Na	500.0	ppm	Ni	50.0	ppm
Rb	30.0	ppm	Sb	0.2	ppm	Sc	0.1	ppm	Se	5.0	ppm
Sn	0.01	%	Sr	0.05	%	Ta	1.0	ppm	Th	0.5	ppm
U	0.05	ppm	W	4.0	ppm	Zn	50.0	ppm	La	1.0	ppm
Ce	3.0	ppm	Nd	5.0	ppm	Sm	0.1	ppm	Eu	0.2	ppm
Tb	0.5	ppm	Yb	0.05	ppm	Lu	0.05	ppm			

X-ray Fluorescence Spectrometry (pressed powder tablets) (Activation Laboratories Ltd.)

Ba	5.0	ppm	Co	5.0	ppm	Cr	5.0	ppm	Cu	5.0	ppm
Ga	5.0	ppm	Nb	2.0	ppm	Ni	5.0	ppm	Pb	5.0	ppm
Rb	2.0	ppm	Sr	2.0	ppm	V	5.0	ppm	Y	2.0	ppm
Zn	5.0	ppm	Zr	5.0	ppm						

Table 3. Selected element concentrations of stream sediment sample 381923 compared with concentrations of stream sediment samples from the Qaqarssuk carbonatite complex (309202, 309356)

GGU no	Fe <sub>2</sub> O <sub>3</sub>	MgO	CaO	Ba	Co	Cr	Cu	Eu	Sr	V
381923	15.05	6.18	7.08	2270	68	469	417	11	762	302
309202	14.43	10.04	11.65	2300	60	98	52	9	1692	176
309356	10.19	7.06	11.97	1200	26	261	38	6	1570	150

**List of figures**

- Fig. 1. Simplified geological map of the survey area. After Allaart (1982)
- Fig. 2. Geochemical map of:  $\text{SiO}_2$  in stream sediment
- Fig. 3. "  $\text{TiO}_2$  "
- Fig. 4. "  $\text{Al}_2\text{O}_3$  "
- Fig. 5. "  $\text{Fe}_2\text{O}_3$  "
- Fig. 6. "  $\text{MnO}$  "
- Fig. 7. "  $\text{MgO}$  "
- Fig. 8. "  $\text{CaO}$  "
- Fig. 9. "  $\text{Na}_2\text{O}$  "
- Fig. 10. "  $\text{K}_2\text{O}$  "
- Fig. 11. "  $\text{P}_2\text{O}_5$  "
- Fig. 12. " As "
- Fig. 13. " Au "
- Fig. 14. " Ba "
- Fig. 15. " Co "
- Fig. 16. " Cr "
- Fig. 17. " Cu "
- Fig. 18. " Ga "
- Fig. 19. " Hf "
- Fig. 20. " Mo "
- Fig. 21. " Nb "
- Fig. 22. " Ni "
- Fig. 23. " Pb "
- Fig. 24. " Rb "
- Fig. 25. " Sb "
- Fig. 26. " Sc "
- Fig. 27. " Sr "
- Fig. 28. " Th "
- Fig. 29. " U "
- Fig. 30. " V "
- Fig. 31. " Y "
- Fig. 32. " Zn "
- Fig. 33. " Zr "
- Fig. 34. " La "
- Fig. 35. " Ce "
- Fig. 36. " Nd "
- Fig. 37. " Sm "
- Fig. 38. " Eu "
- Fig. 39. " Yb "
- Fig. 40. " Lu "
- Fig. 41. Map of gamma-radiation
- Fig. 42. Conductivity of stream water
- Fig. 43. Geochemical map of fluoride in stream water
- Fig. 44. Stream sediment anomalies

GEOLOGICAL MAP

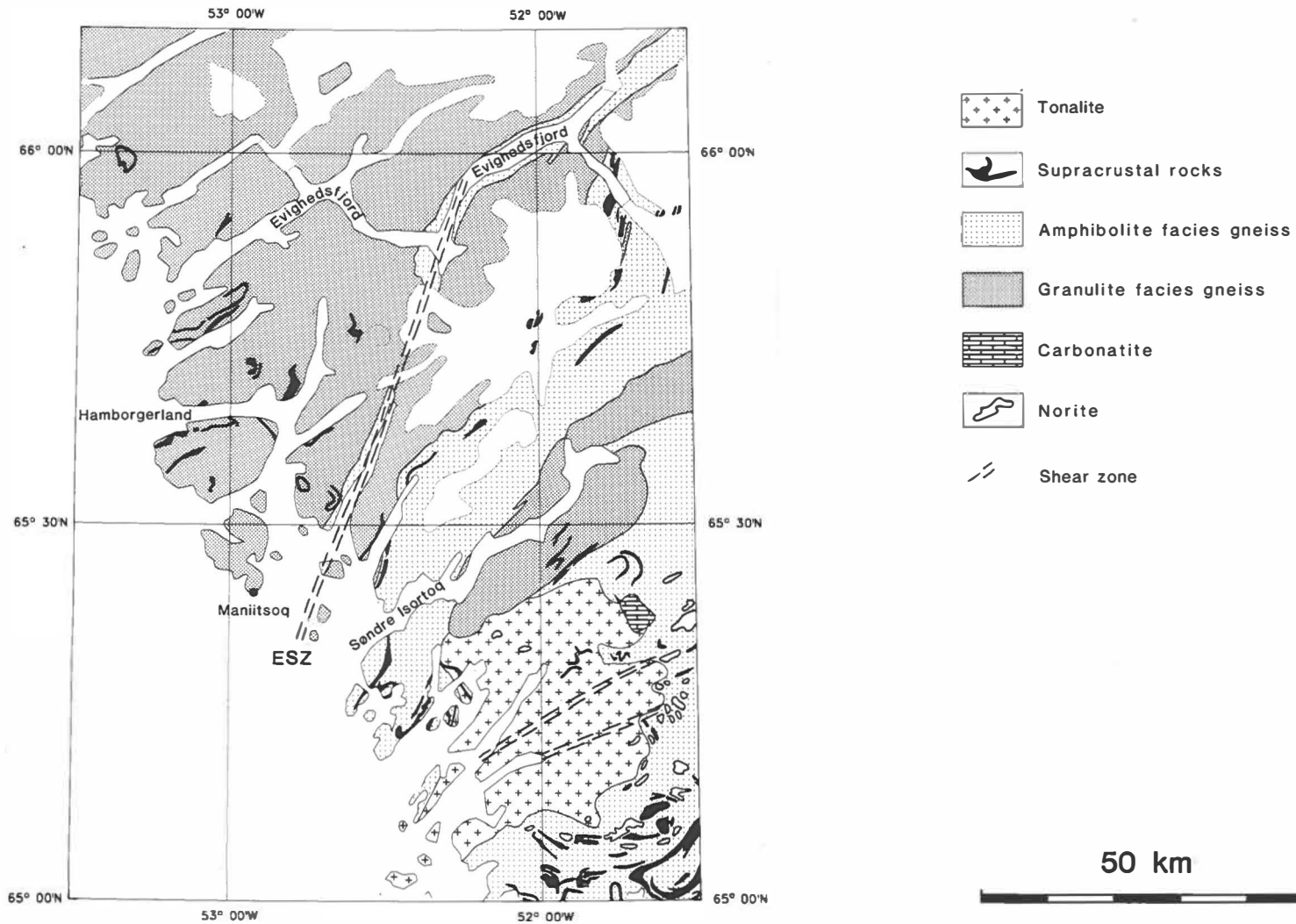
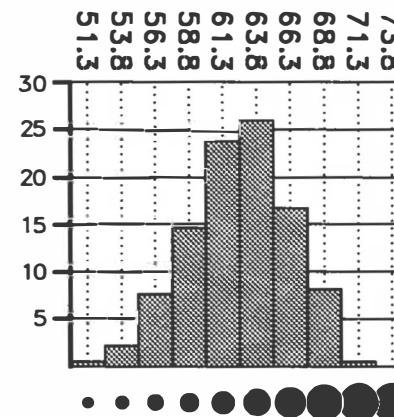
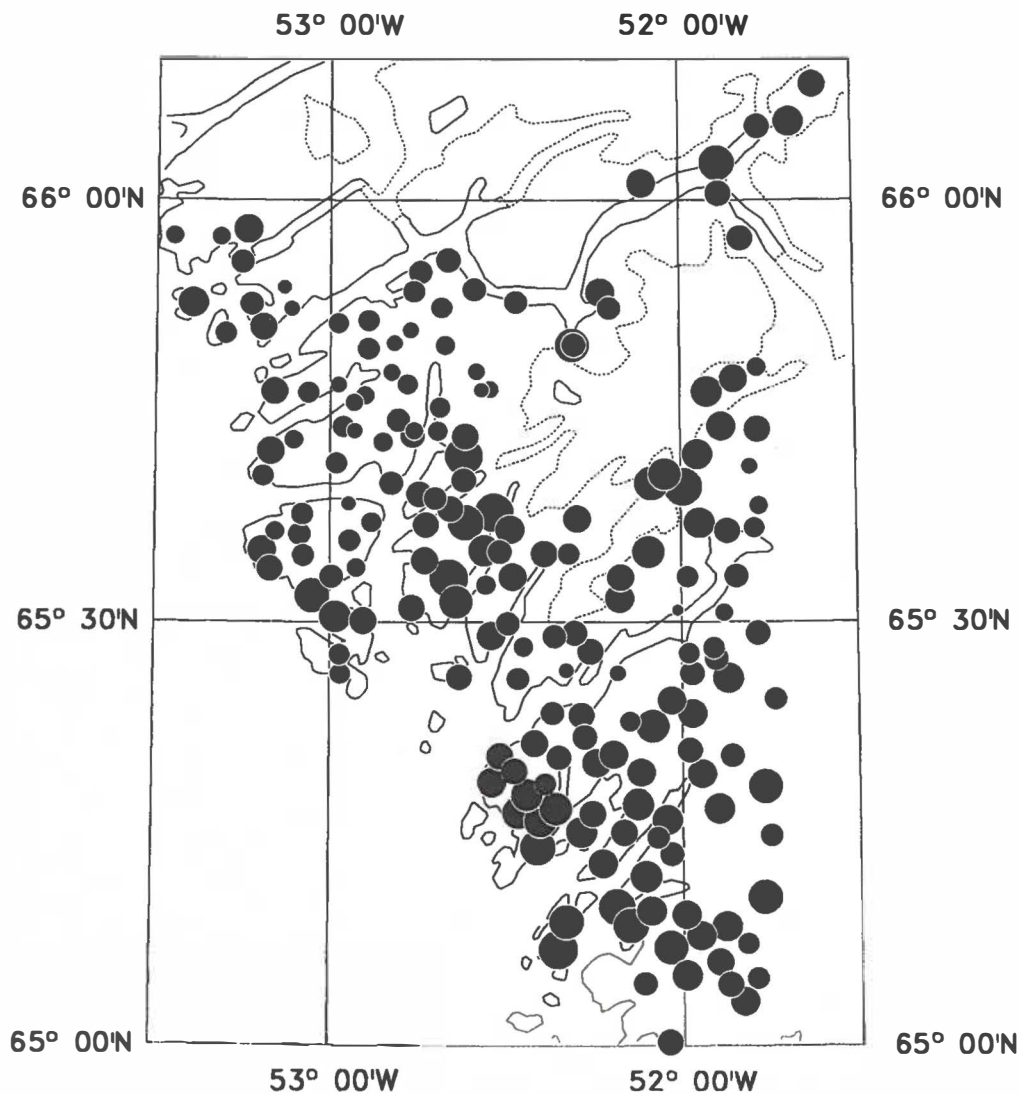


Fig. 1



# SiO<sub>2</sub> in stream sediment

Fig. 2



SiO<sub>2</sub> pct

X-ray Fluorescence

Number of samples:	185
Min. value:	50.9
Max. value:	70.2
Mean:	62.5
Median:	62.7
Variance:	13.6
Std. Dev.:	3.7

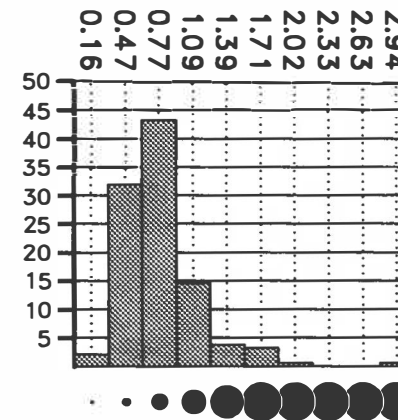
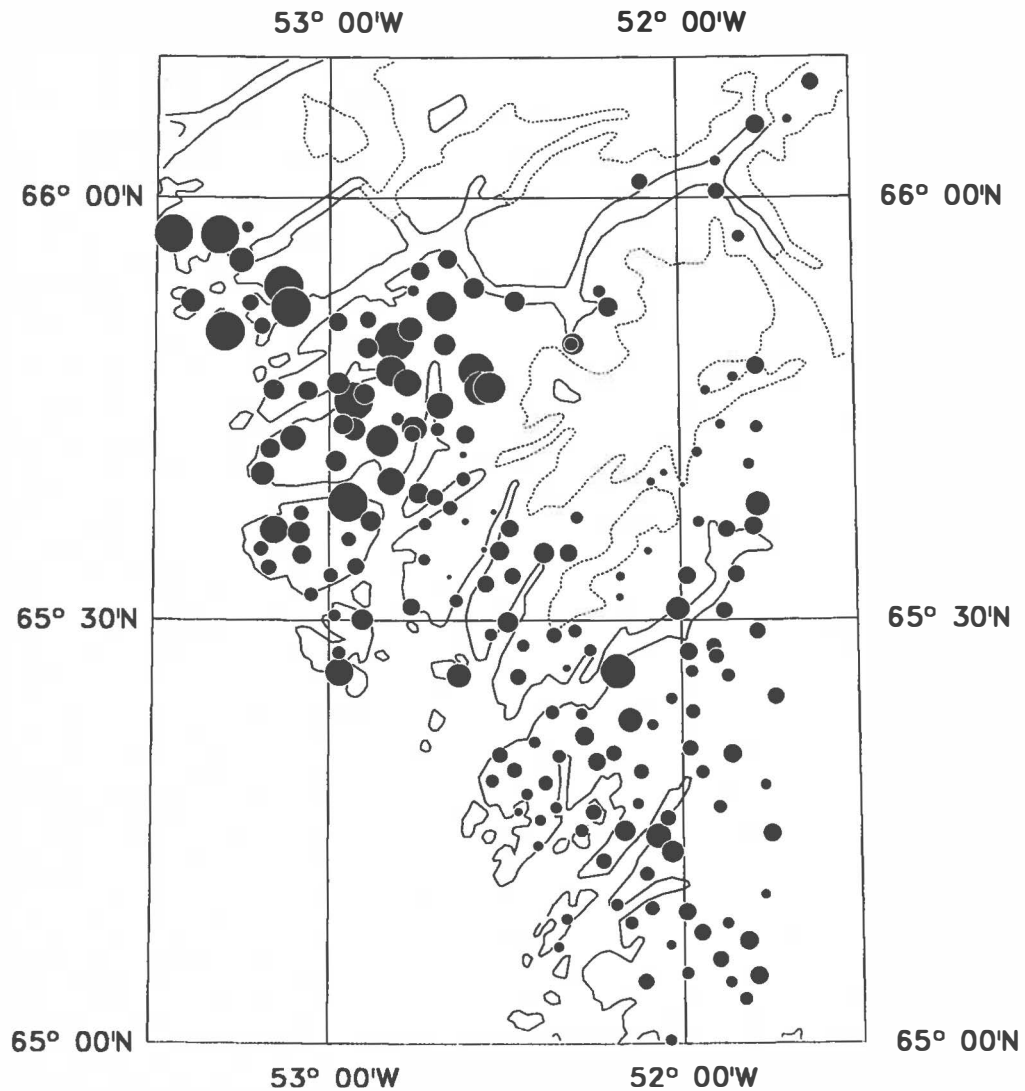
50 km





# TiO<sub>2</sub> in stream sediment

Fig. 3



TiO<sub>2</sub> pct

X-ray Fluorescence

Number of samples:	185
Min. value:	0.27
Max. value:	3.04
Mean:	0.80
Median:	0.74
Variance:	0.11
Std. Dev.:	0.34

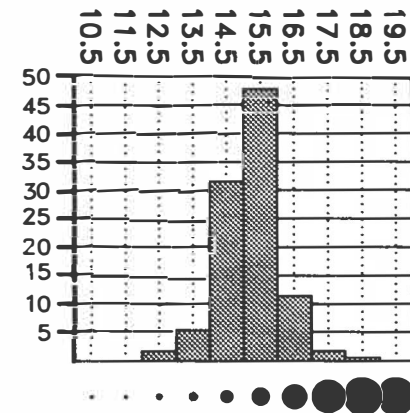
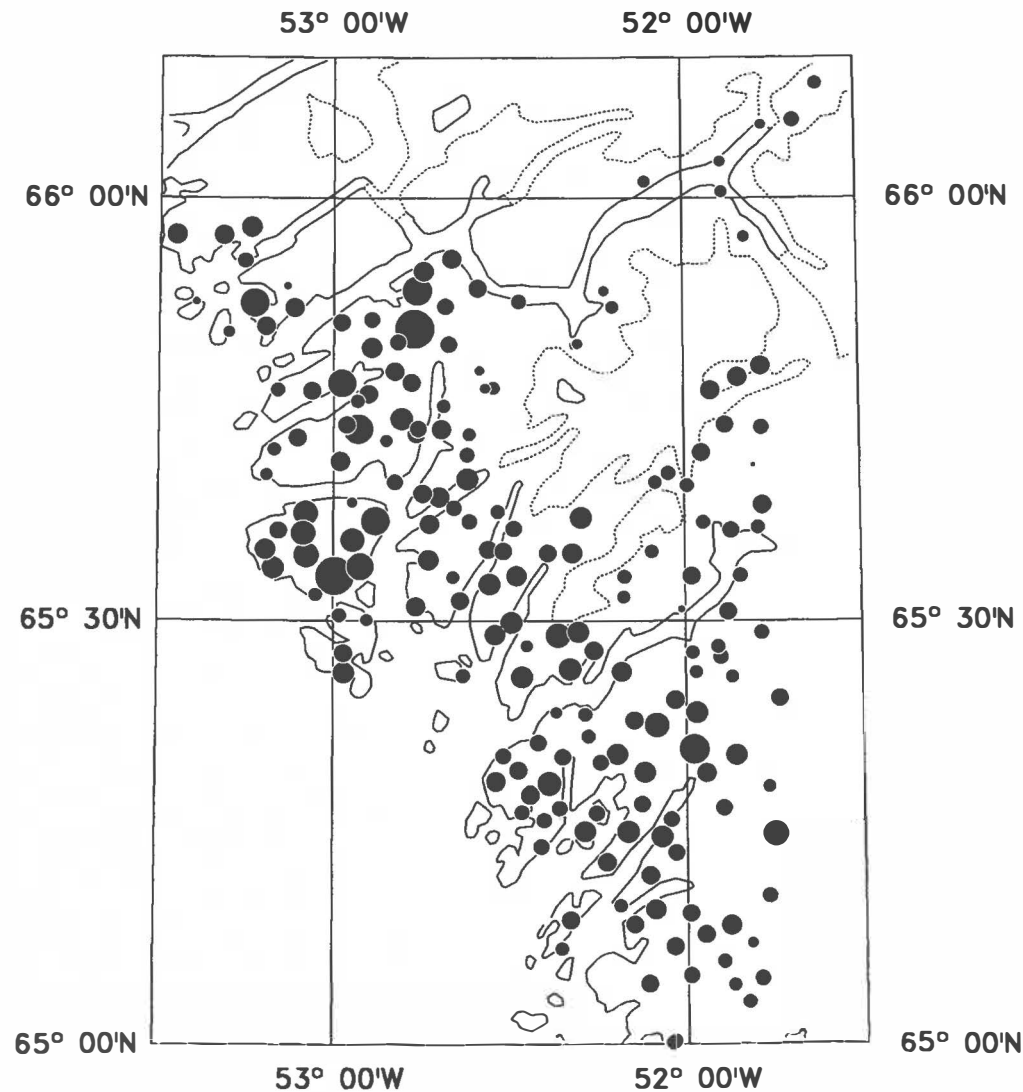
50 km





# Al<sub>2</sub>O<sub>3</sub> in stream sediment

Fig. 4



Al<sub>2</sub>O<sub>3</sub> pct

X-ray Fluorescence

Number of samples:	185
Min. value:	9.9
Max. value:	18.6
Mean:	15.2
Median:	15.2
Variance:	0.9
Std. Dev.:	0.9

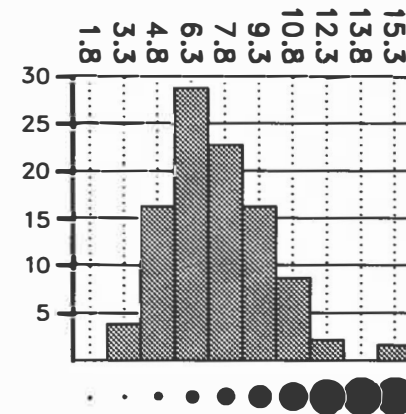
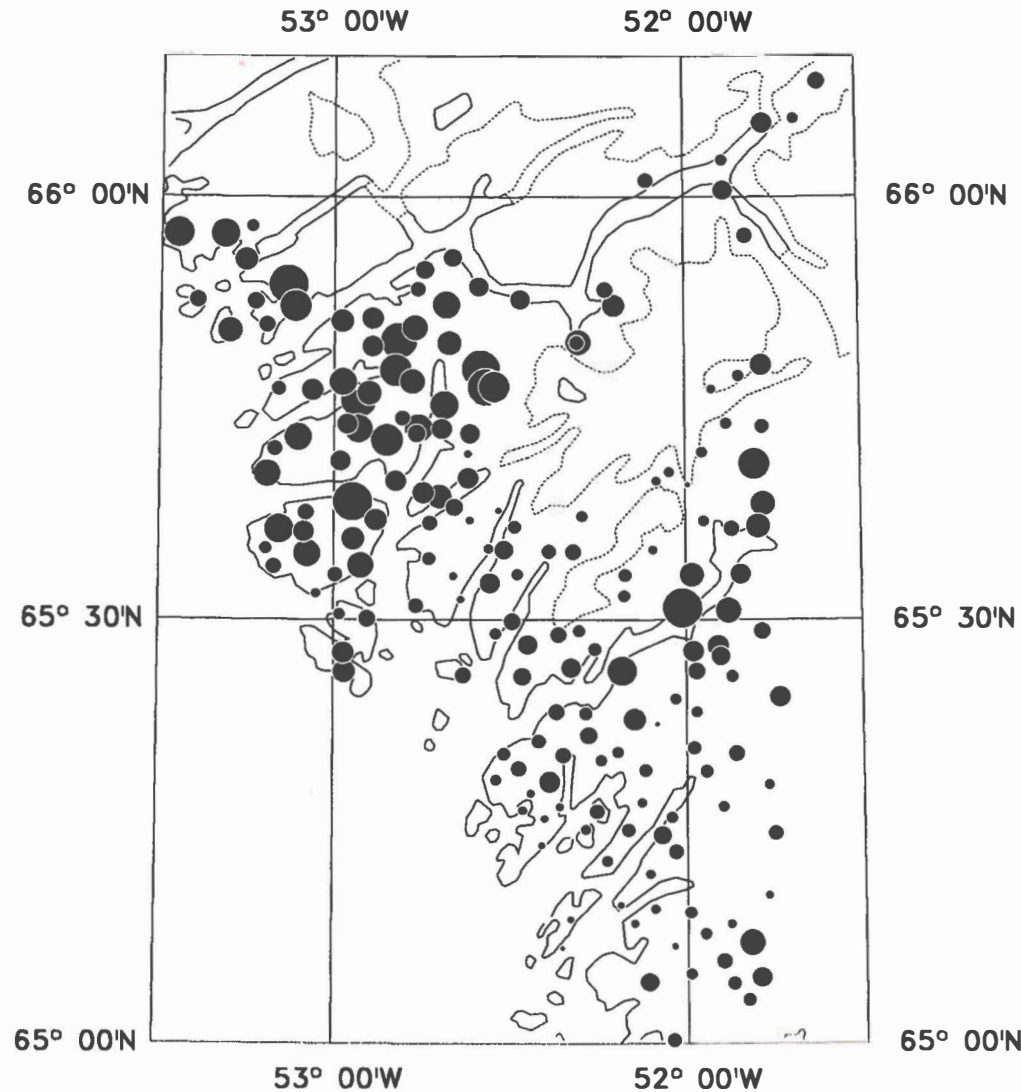
50 km





# Fe2O3 in stream sediment

Fig. 5



Fe<sub>2</sub>O<sub>3</sub> pct

X-ray Fluorescence

Number of samples:	185
Min. value:	3.0
Max. value:	15.4
Mean:	7.4
Median:	7.1
Variance:	5.1
Std. Dev.:	2.3

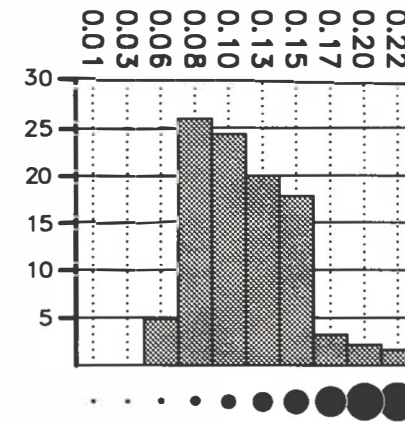
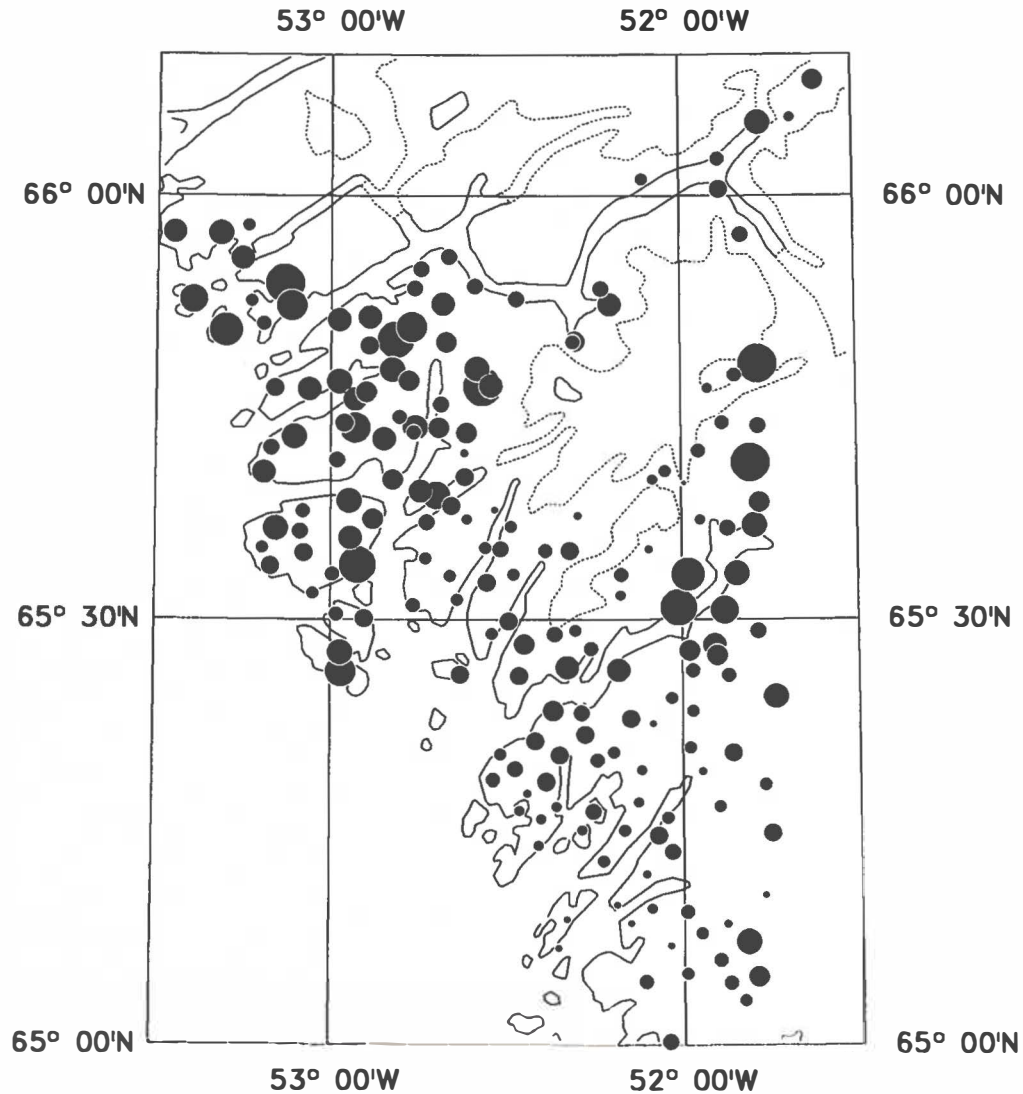
50 km





MnO in stream sediment

Fig. 6



MnO pct

X-ray Fluorescence

Number of samples:	185
Min. value:	0.05
Max. value:	0.22
Mean:	0.11
Median:	0.11
Variance:	0.00
Std. Dev.:	0.03

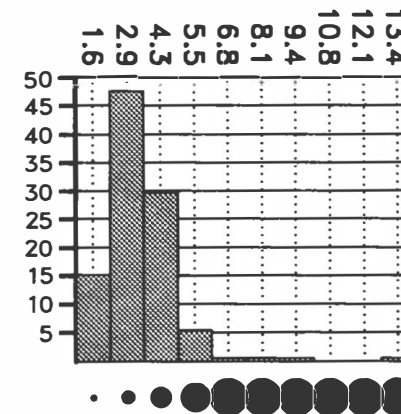
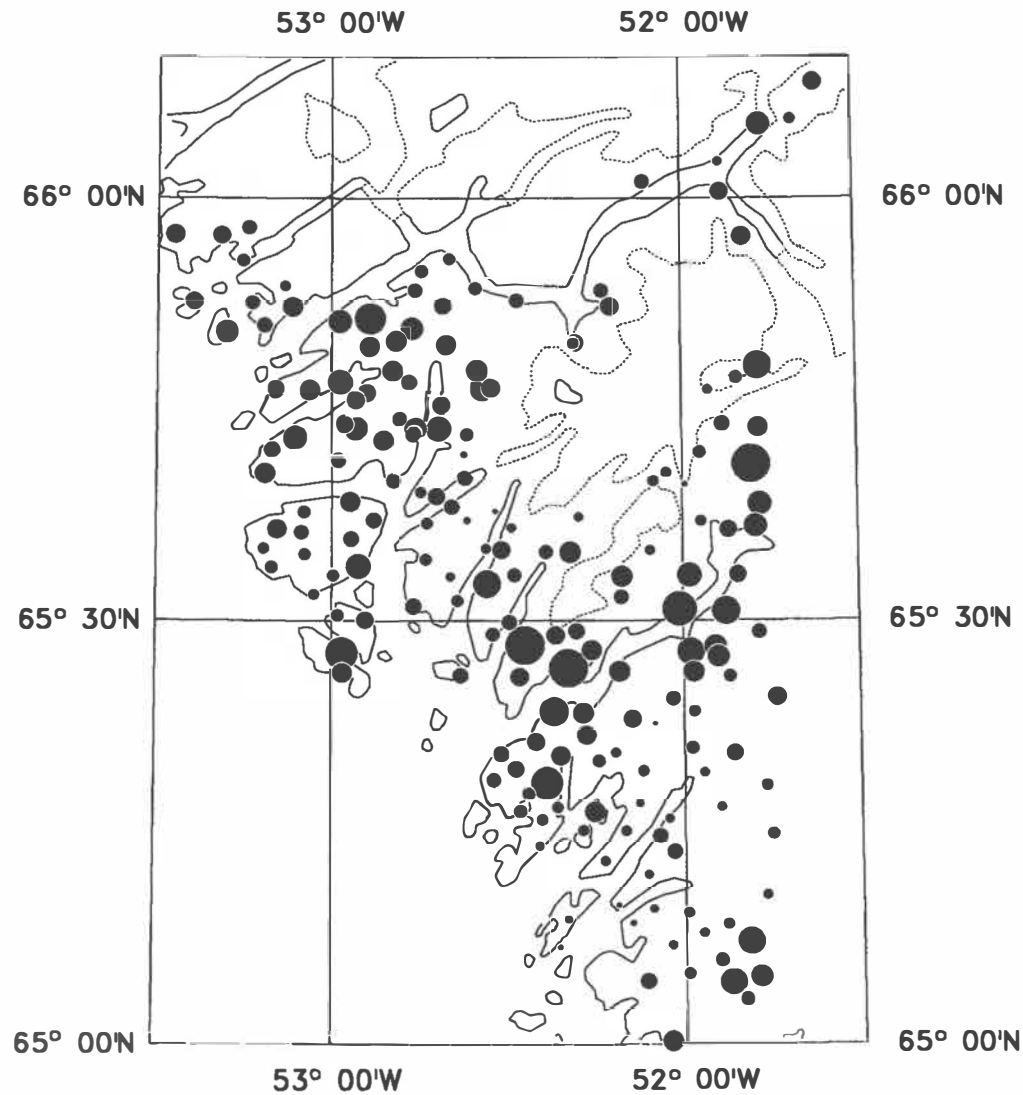
50 km





# MgO in stream sediment

Fig. 7



MgO pct

X-ray Fluorescence

Number of samples:	185
Min. value:	1.2
Max. value:	13.1
Mean:	3.4
Median:	3.2
Variance:	1.8
Std. Dev.:	1.4

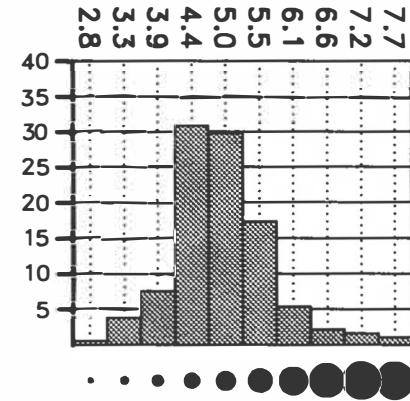
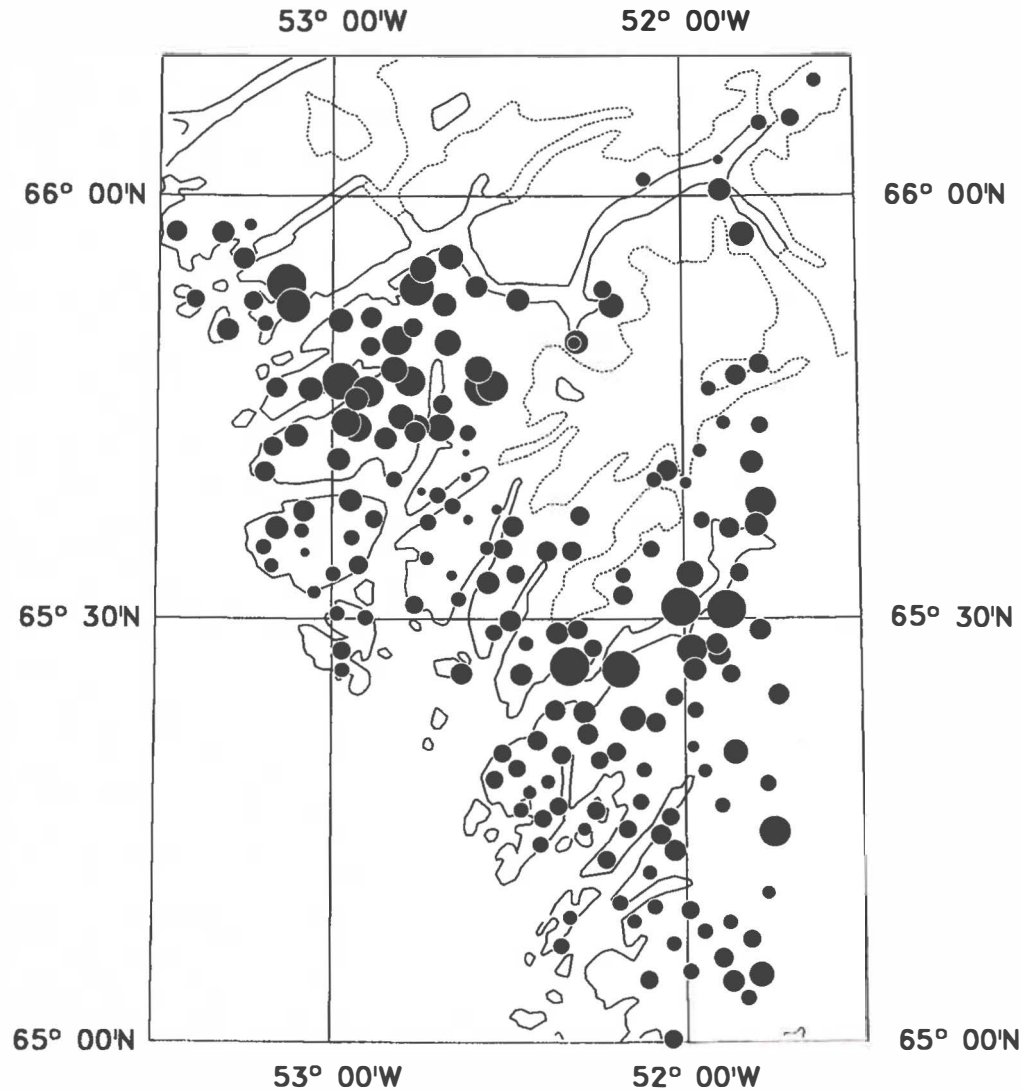
50 km





CaO in stream sediment

Fig. 8



CaO pct

X-ray Fluorescence

Number of samples:	185
Min. value:	3.0
Max. value:	7.6
Mean:	4.9
Median:	4.8
Variance:	0.6
Std. Dev.:	0.8

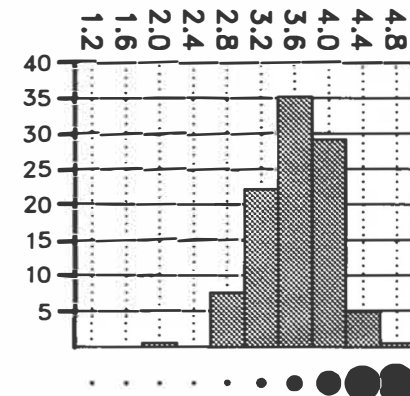
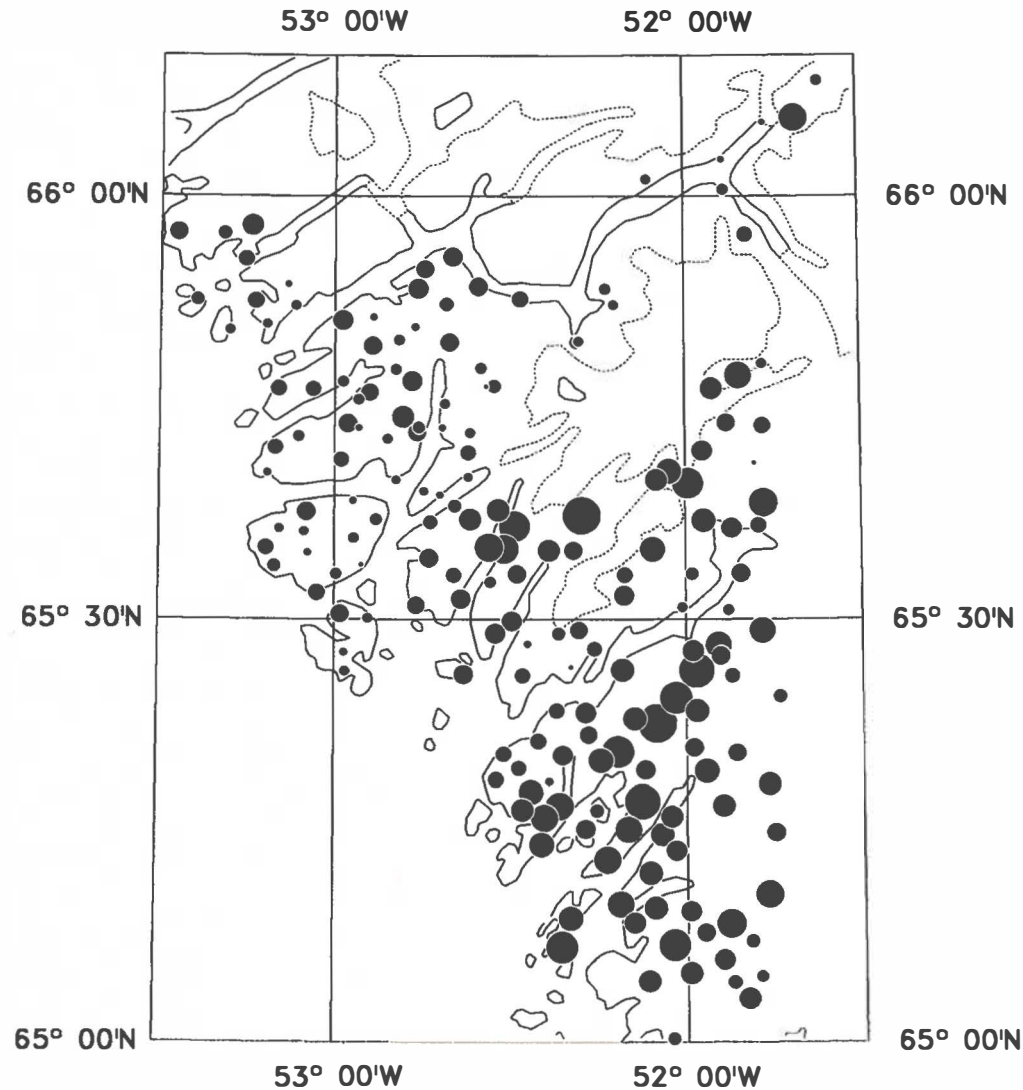
50 km





# Na<sub>2</sub>O in stream sediment

Fig. 9



Na<sub>2</sub>O pct  
AAS

Number of samples:	185
Min. value:	2.0
Max. value:	4.6
Mean:	3.6
Median:	3.7
Variance:	0.2
Std. Dev.:	0.4

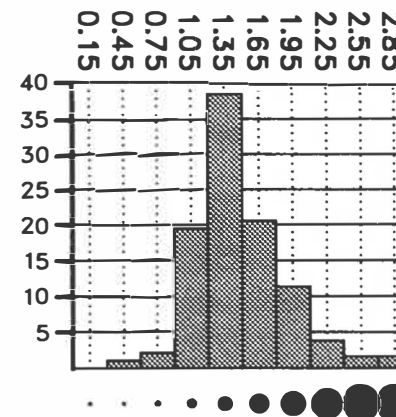
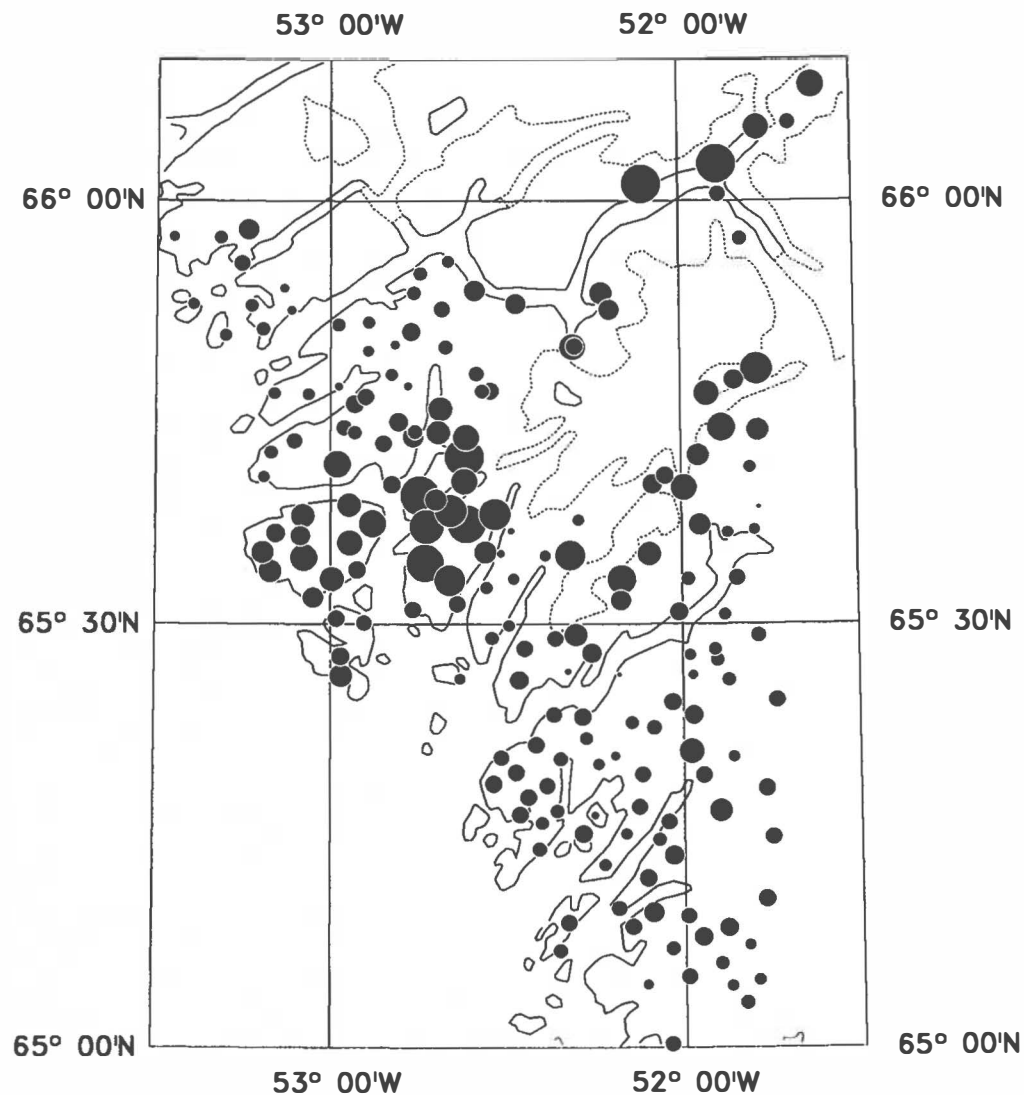
50 km





# K20 in stream sediment

Fig. 10



K20 pct

X-ray Fluorescence

Number of samples:	185
Min. value:	0.56
Max. value:	2.83
Mean:	1.49
Median:	1.44
Variance:	0.16
Std. Dev.:	0.39

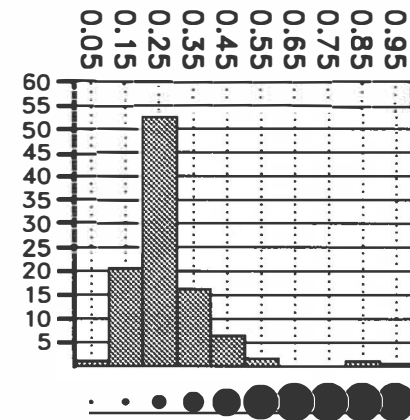
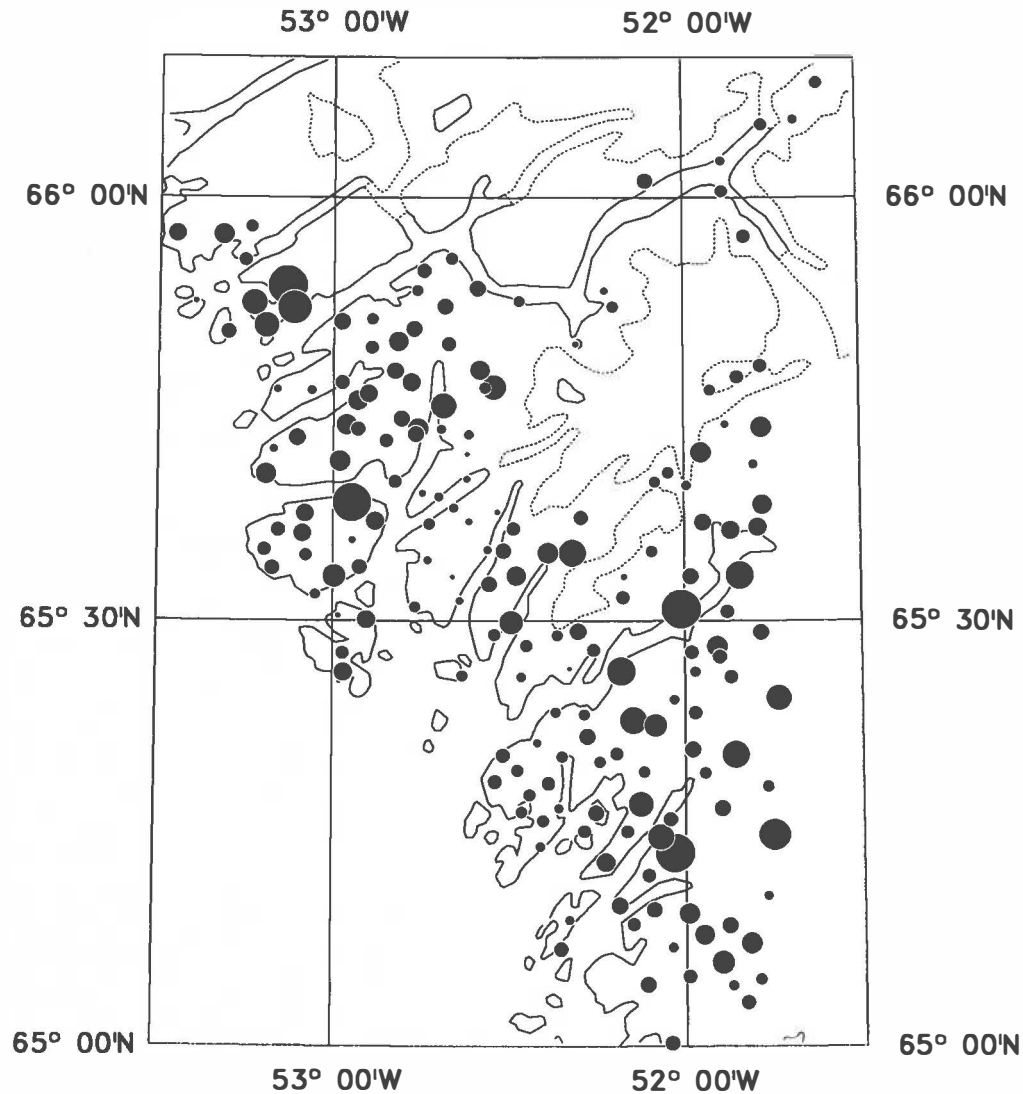
50 km





# P205 in stream sediment

Fig. 11



P205 pct

X-ray Fluorescence

Number of samples:	185
Min. value:	0.08
Max. value:	0.96
Mean:	0.27
Median:	0.25
Variance:	0.01
Std. Dev.:	0.12

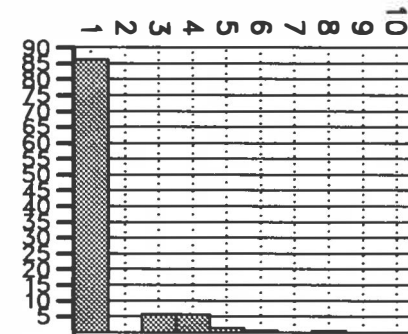
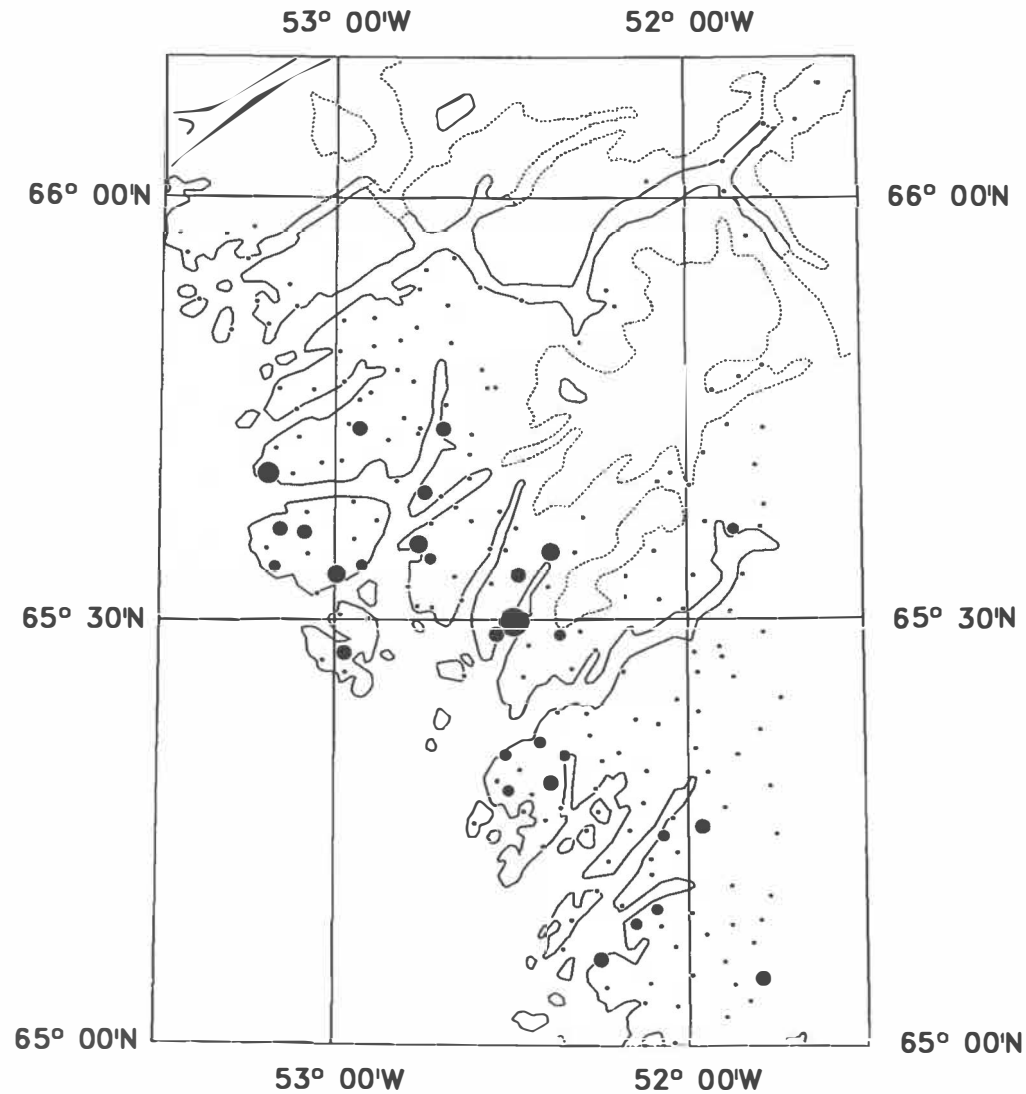
50 km





# As in stream sediment

Fig. 12



As ppm

INAA

Number of samples:	211
Min. value:	0
Max. value:	7
Mean:	0
Median:	0
Variance:	1
Std. Dev.:	1

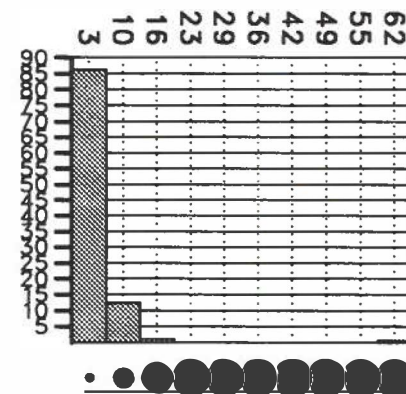
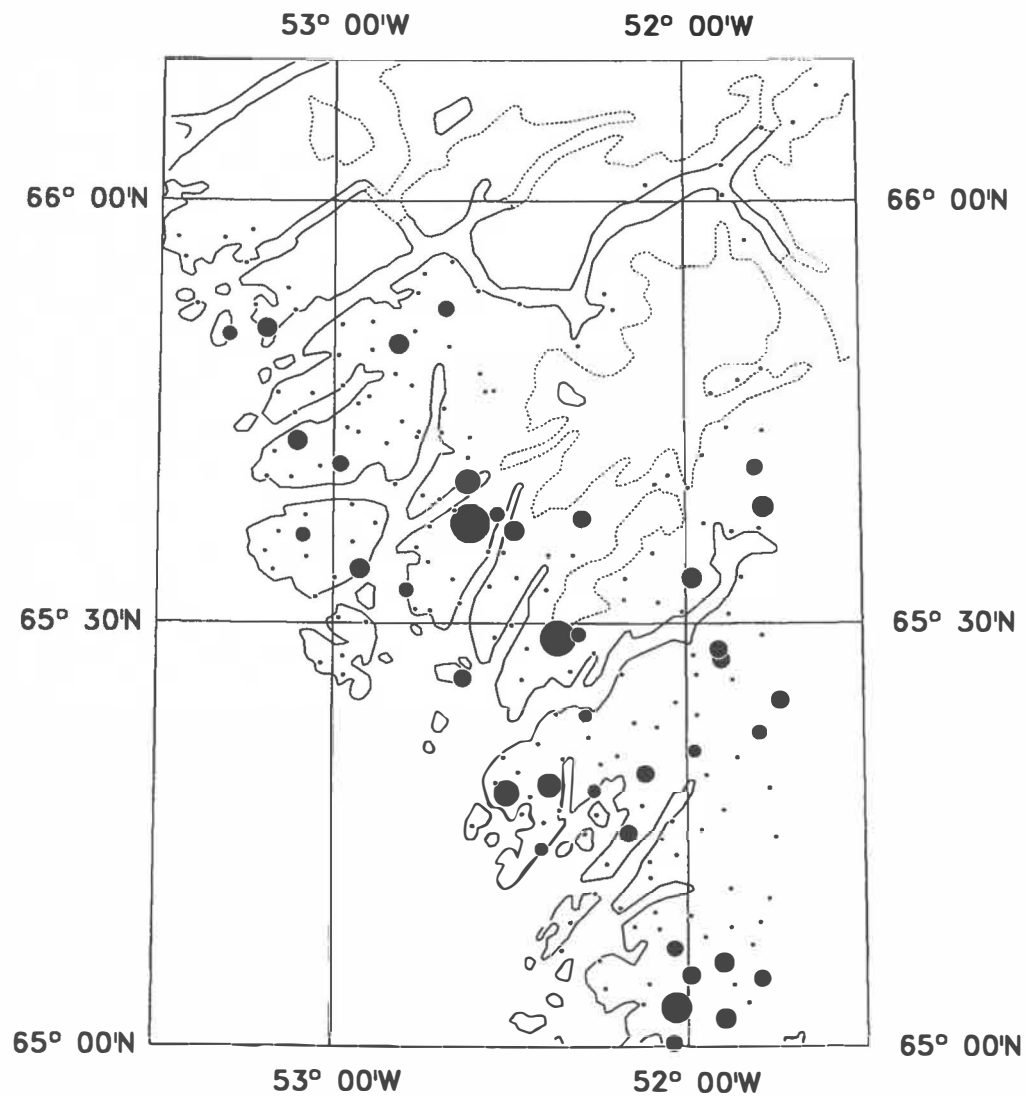
50 km





# Au in stream sediment

Fig. 13



Au ppb

NAA

Number of samples:	211
Min. value:	0
Max. value:	61
Mean:	2
Median:	0
Variance:	28
Std. Dev.:	5

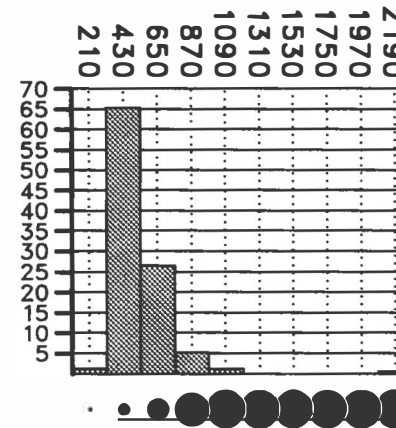
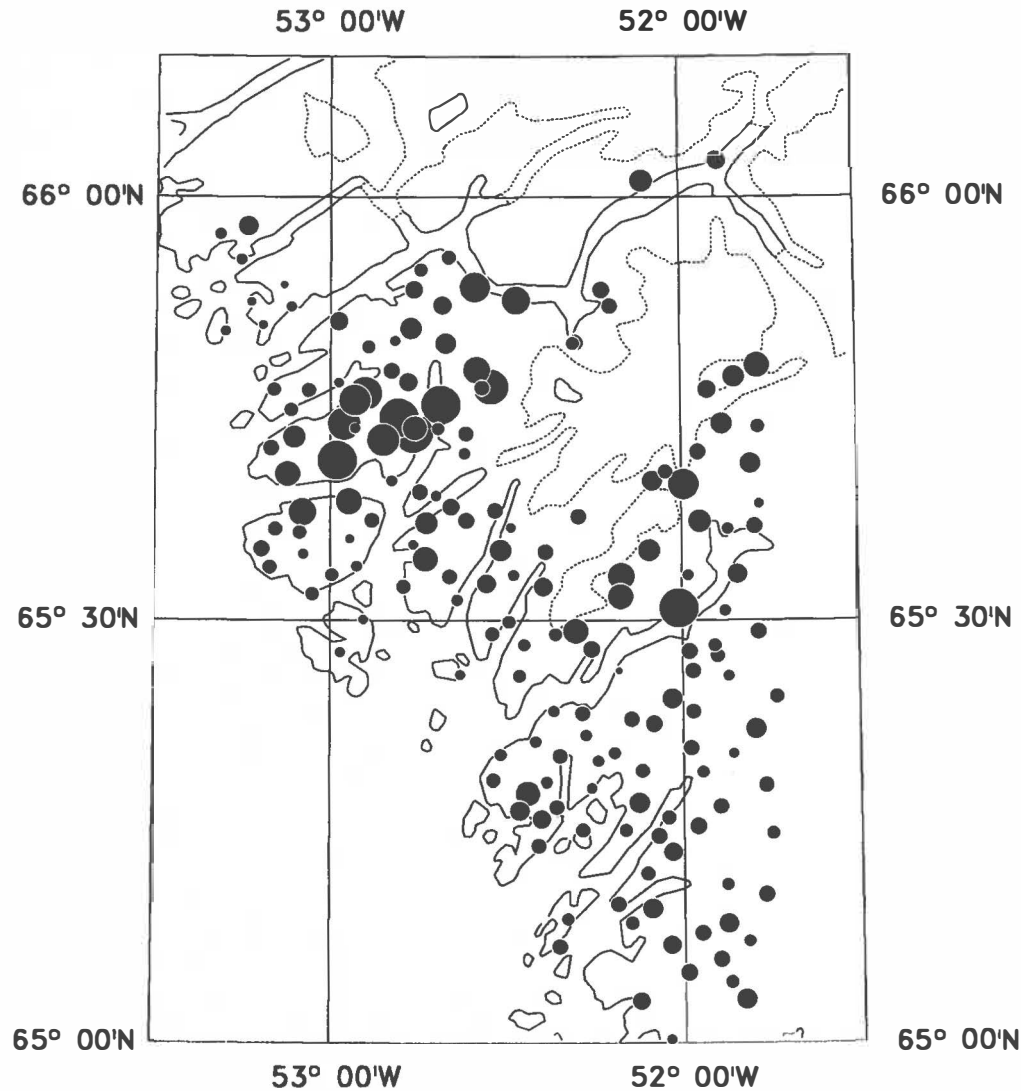
50 km





# Ba in stream sediment

Fig. 14



Ba ppm

X-ray Fluorescence

Number of samples:	173
Min. value:	293
Max. value:	2270
Mean:	537
Median:	497
Variance:	36562
Std. Dev.:	191

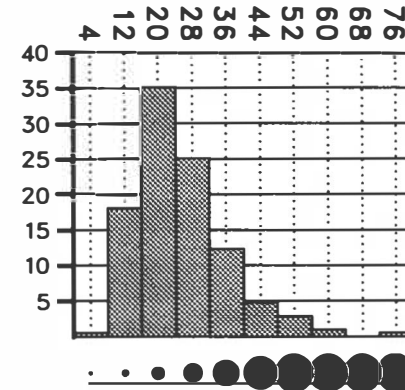
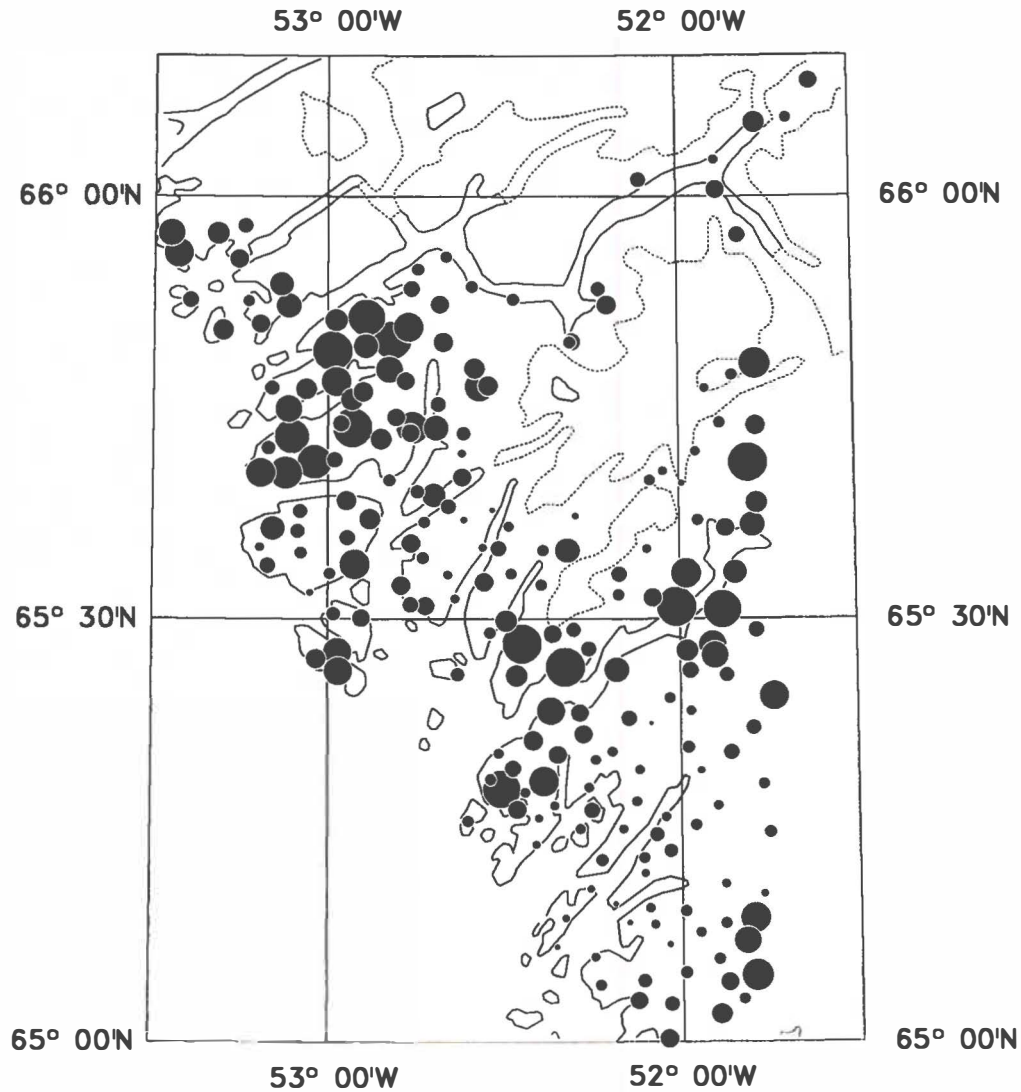
50 km





# Co in stream sediment

Fig. 15



Co ppm  
INAA

Number of samples:	211
Min. value:	7
Max. value:	75
Mean:	25
Median:	23
Variance:	113
Std. Dev.:	11

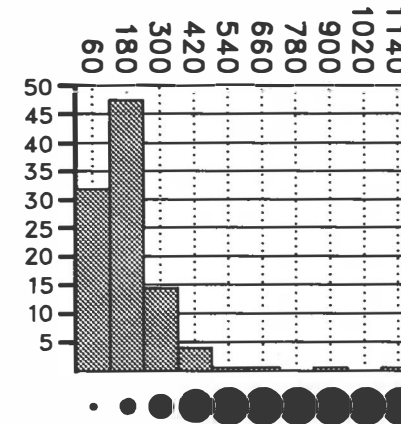
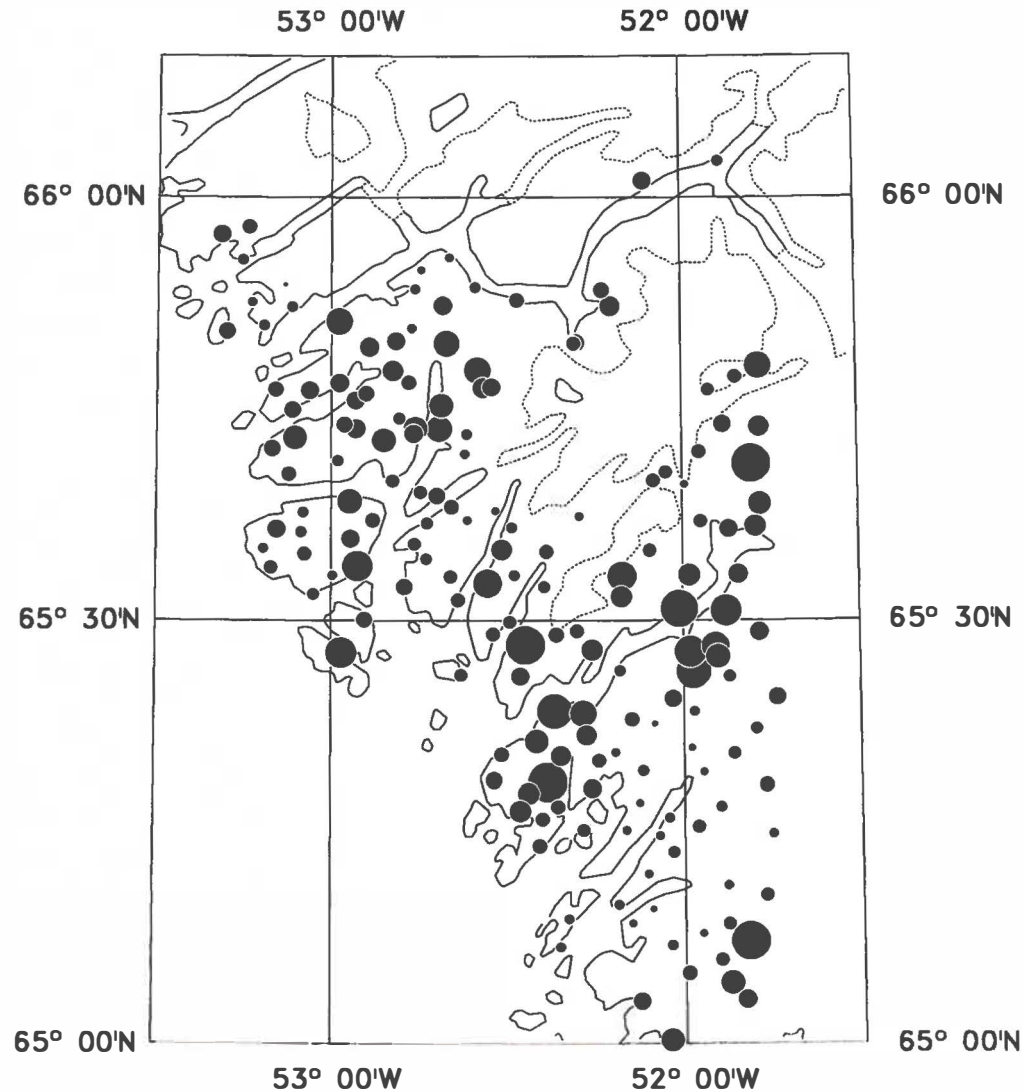
50 km





# Cr in stream sediment

Fig. 16



Cr ppm

X-ray Fluorescence

Number of samples:	173
Min. value:	12
Max. value:	1144
Mean:	185
Median:	149
Variance:	19133
Std. Dev.:	138

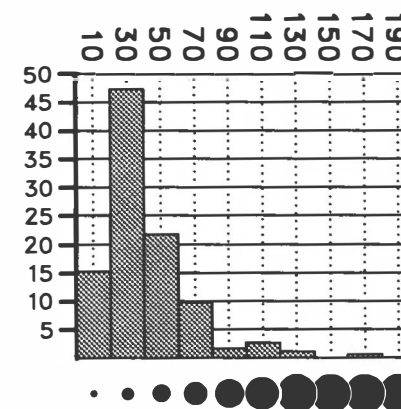
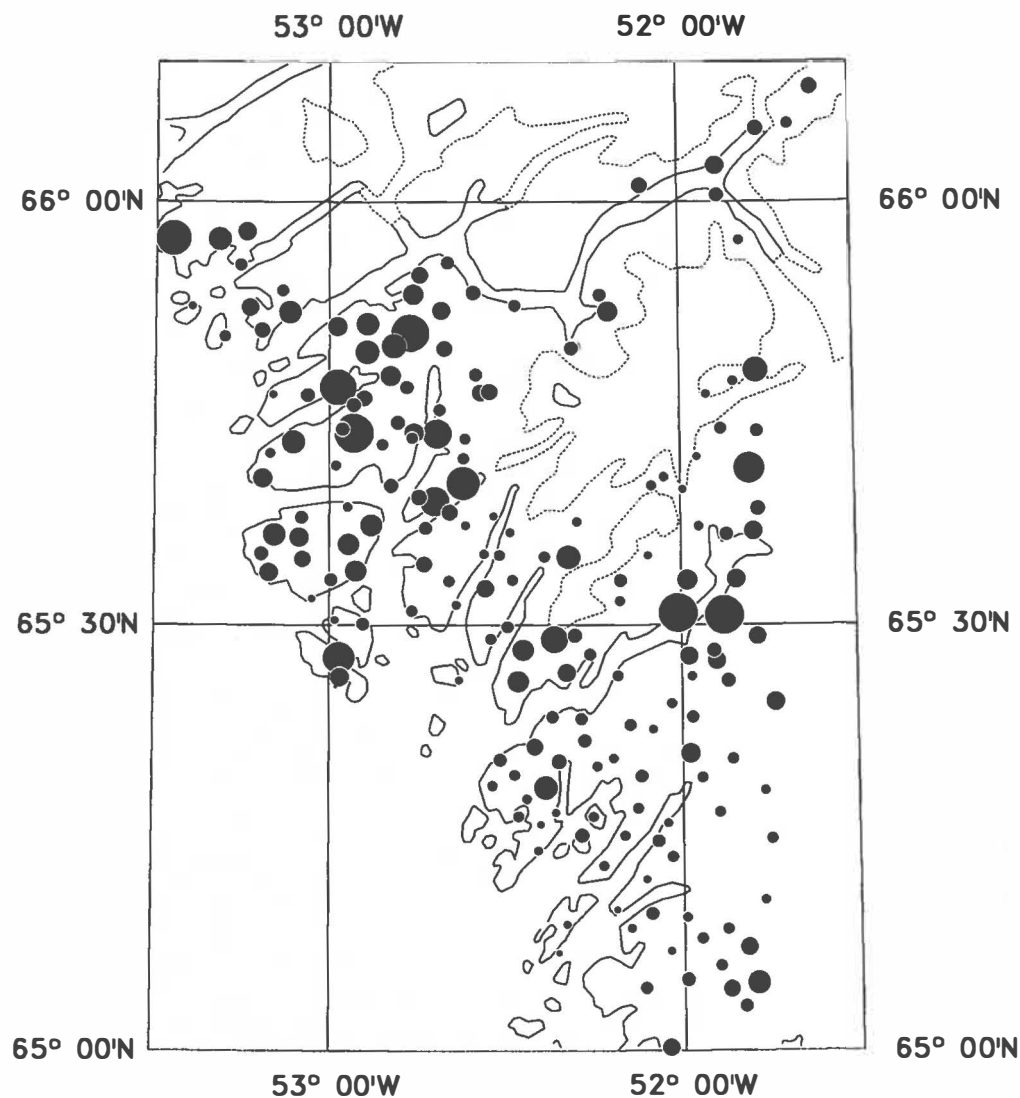
50 km





# Cu in stream sediment

Fig. 17



Cu ppm

AAS

Number of samples:	185
Min. value:	8
Max. value:	383
Mean:	42
Median:	33
Variance:	1259
Std. Dev.:	35

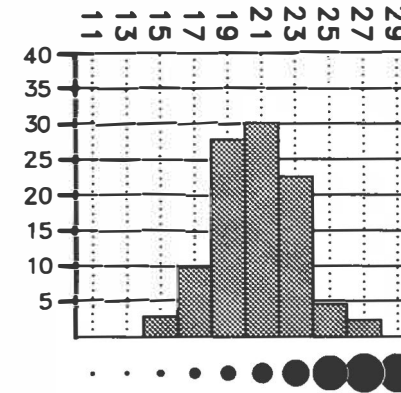
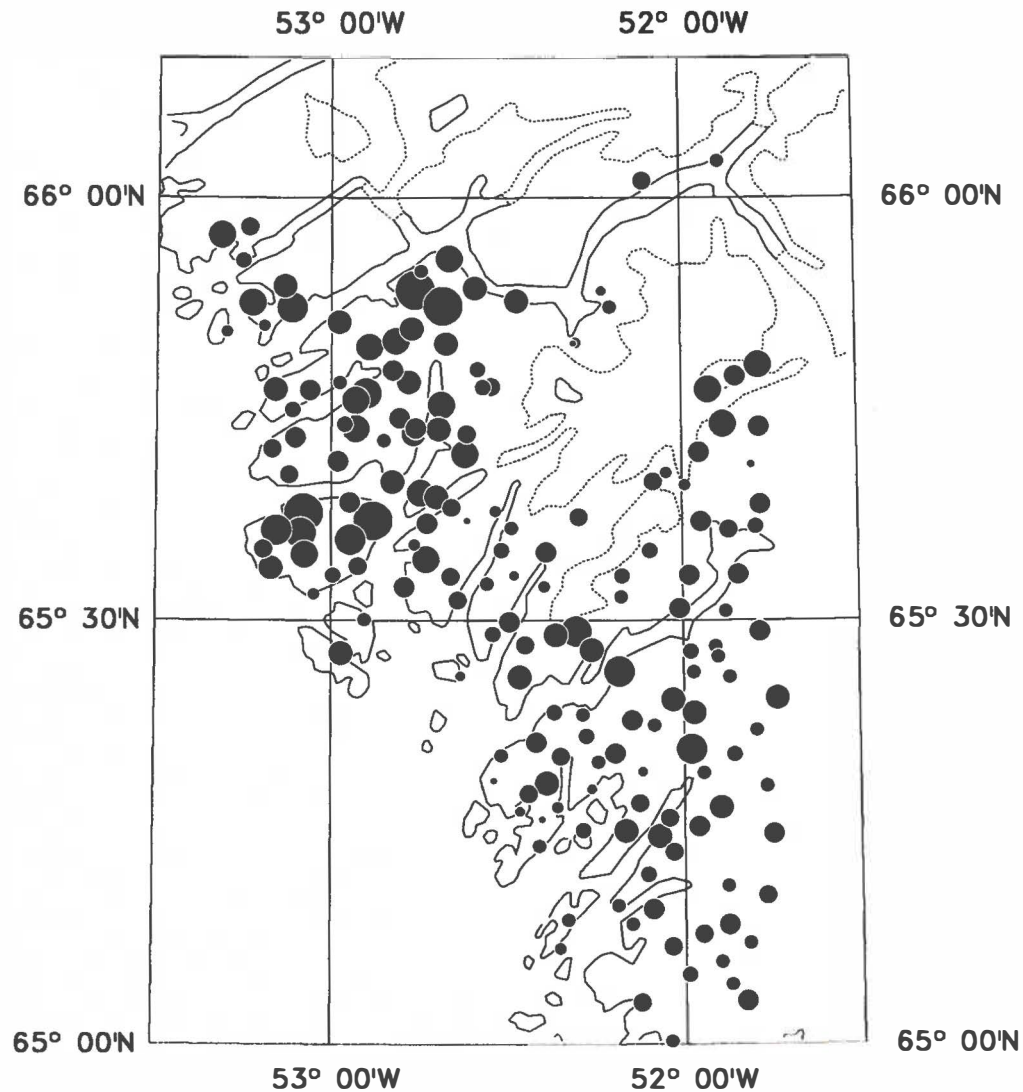
50 km





# Ga in stream sediment

Fig. 18



Ga ppm

X-ray Fluorescence

Number of samples:	173
Min. value:	14
Max. value:	26
Mean:	20
Median:	20
Variance:	6
Std. Dev.:	2

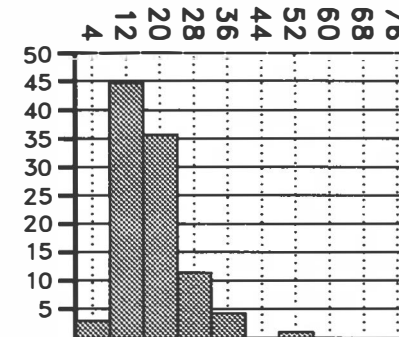
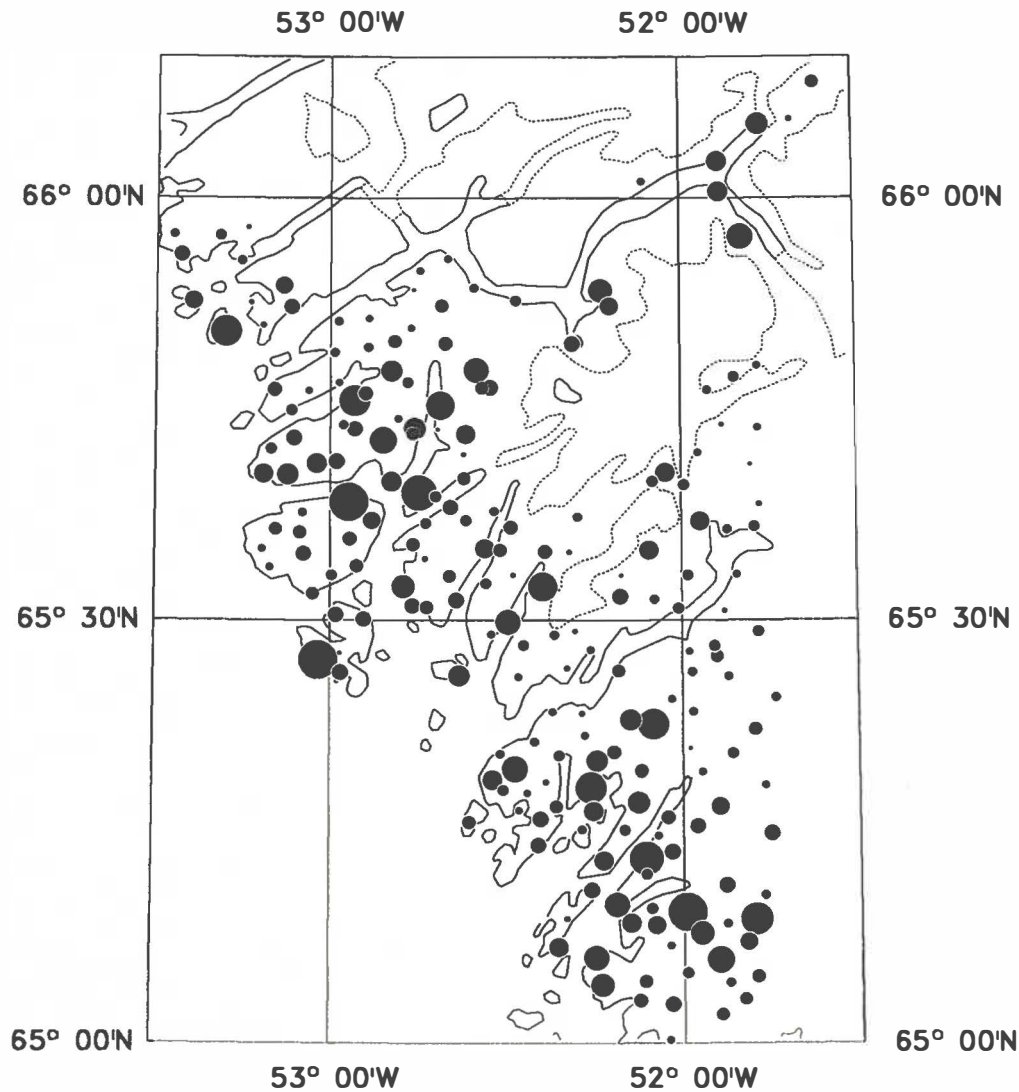
50 km





# Hf in stream sediment

Fig. 19



Hf ppm  
INAA

Number of samples:	211
Min. value:	3
Max. value:	80
Mean:	18
Median:	16
Variance:	77
Std. Dev.:	9

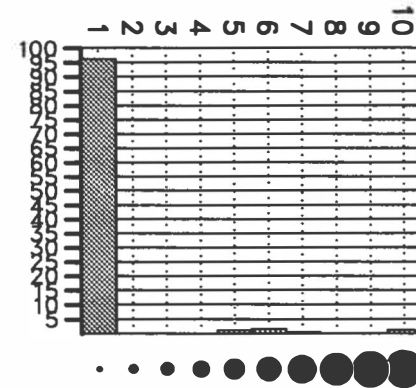
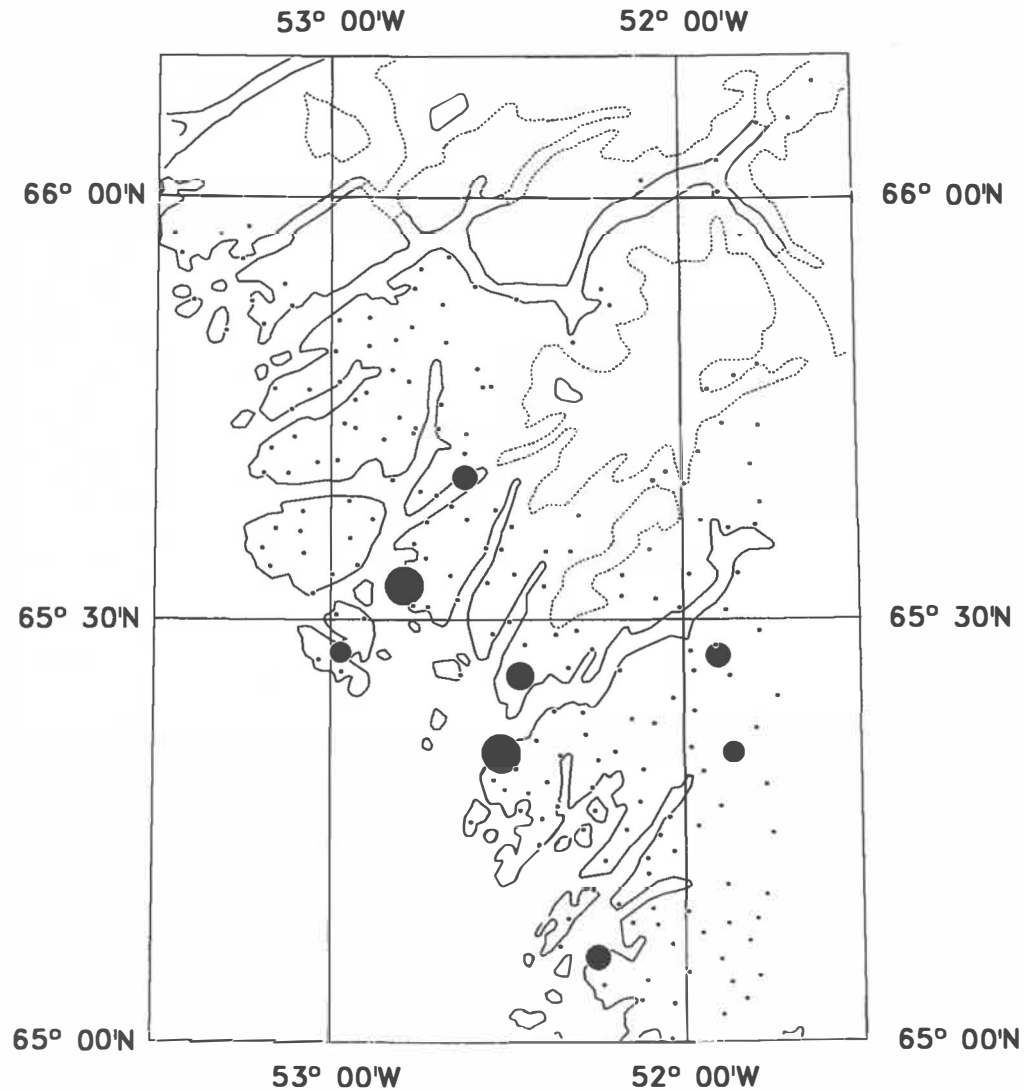
50 km





# Mo in stream sediment

Fig. 20



Mo ppm  
INAA

Number of samples:	211
Min. value:	0
Max. value:	10
Mean:	0
Median:	0
Variance:	2
Std. Dev.:	1

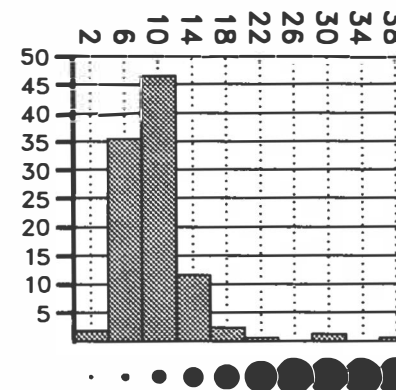
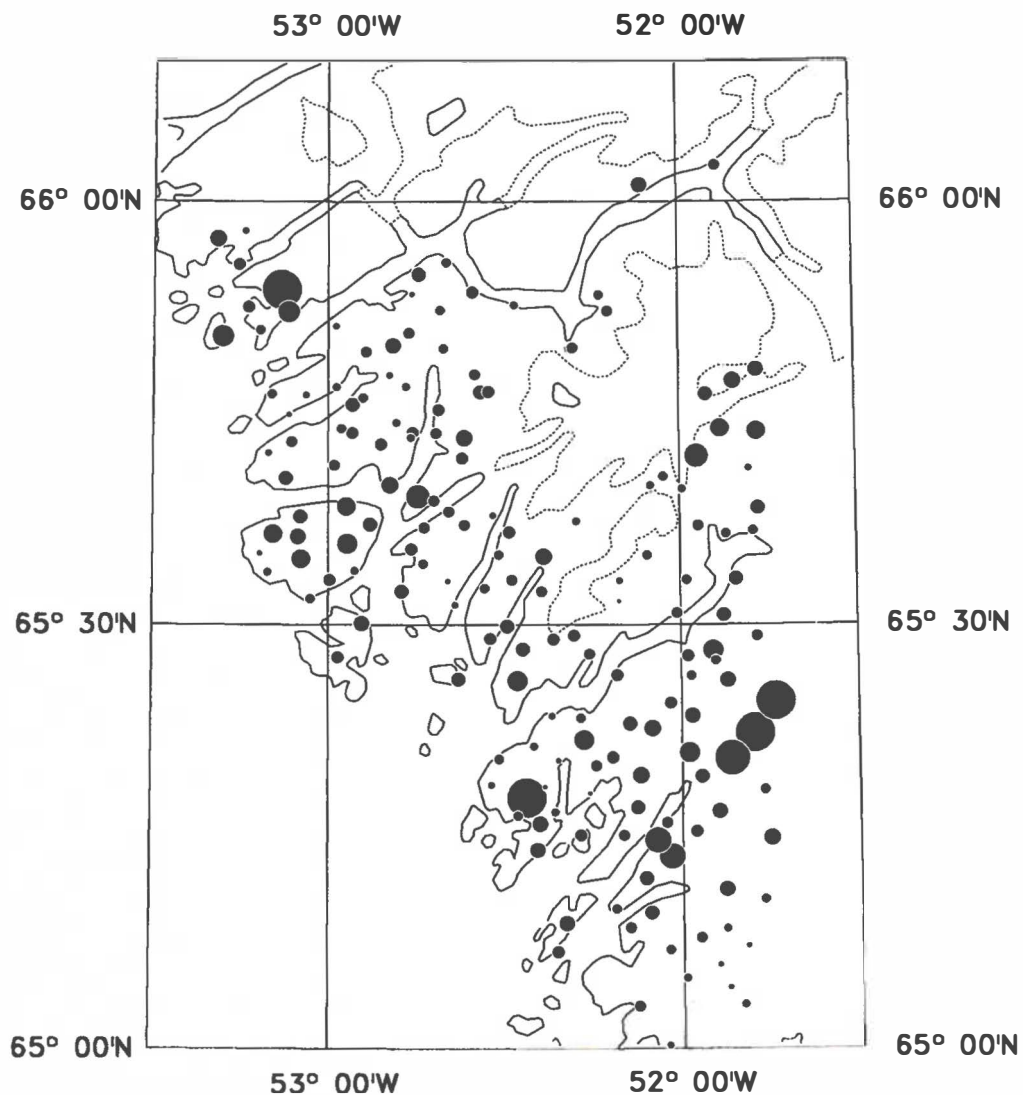
50 km





# Nb in stream sediment

Fig. 21



Nb ppm

X-ray Fluorescence

Number of samples:	173
Min. value:	2
Max. value:	88
Mean:	10
Median:	8
Variance:	55
Std. Dev.:	7

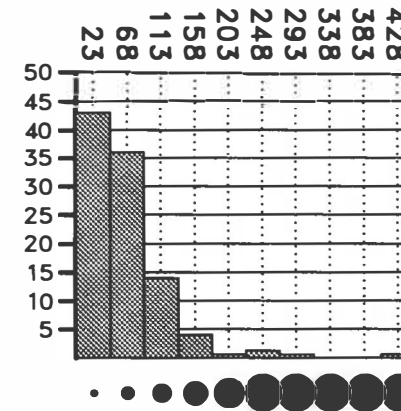
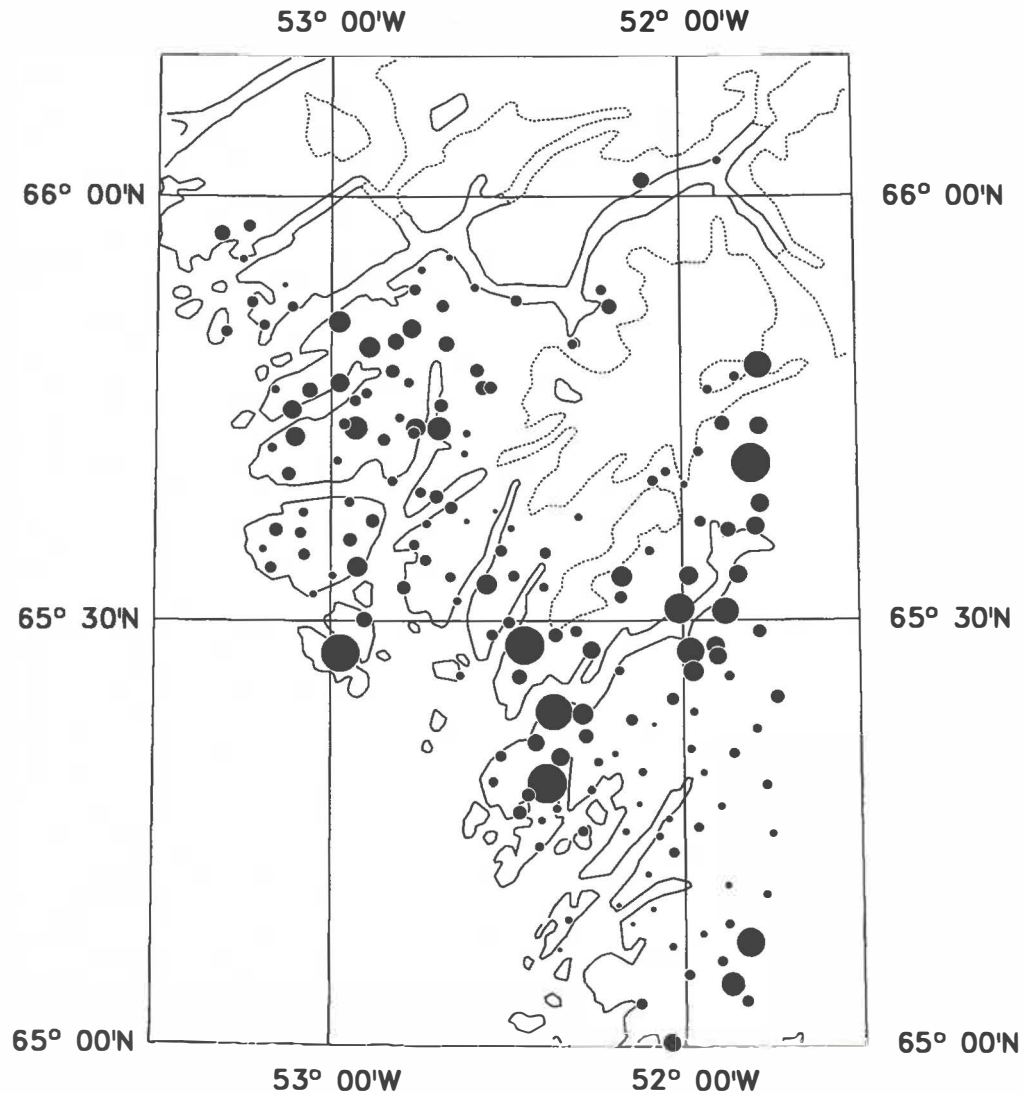
50 km





Ni in stream sediment

Fig. 22



Ni ppm

X-ray Fluorescence

Number of samples:	173
Min. value:	0
Max. value:	783
Mean:	68
Median:	49
Variance:	5923
Std. Dev.:	77

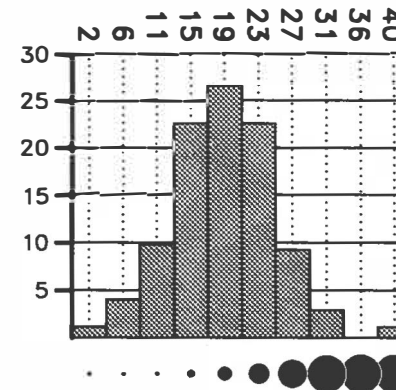
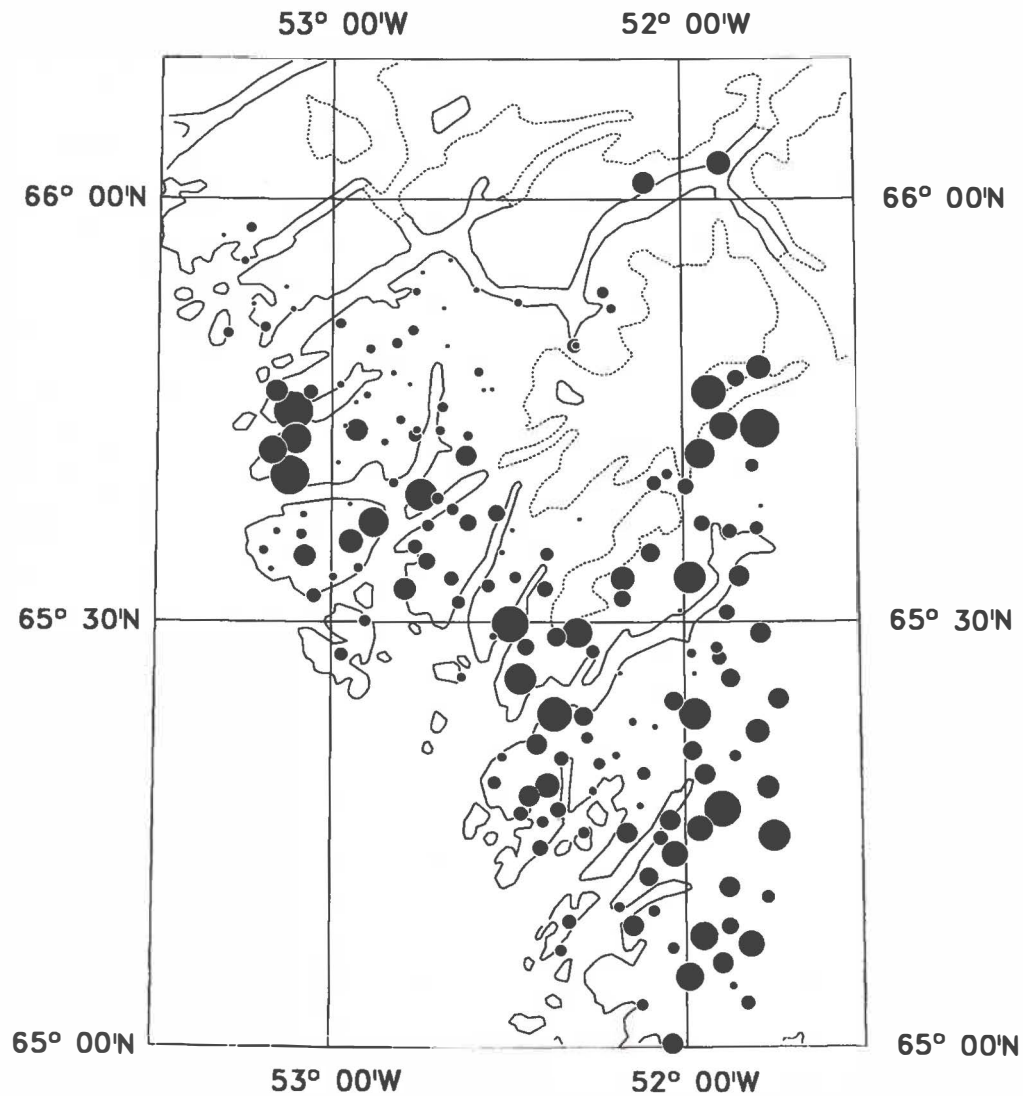
50 km





Pb in stream sediment

Fig. 23



Pb ppm

X-ray Fluorescence

Number of samples:	173
Min. value:	0
Max. value:	40
Mean:	19
Median:	18
Variance:	42
Std. Dev.:	6

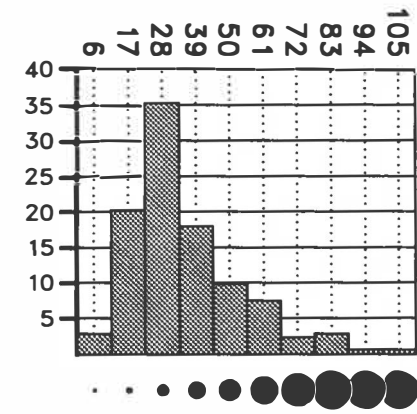
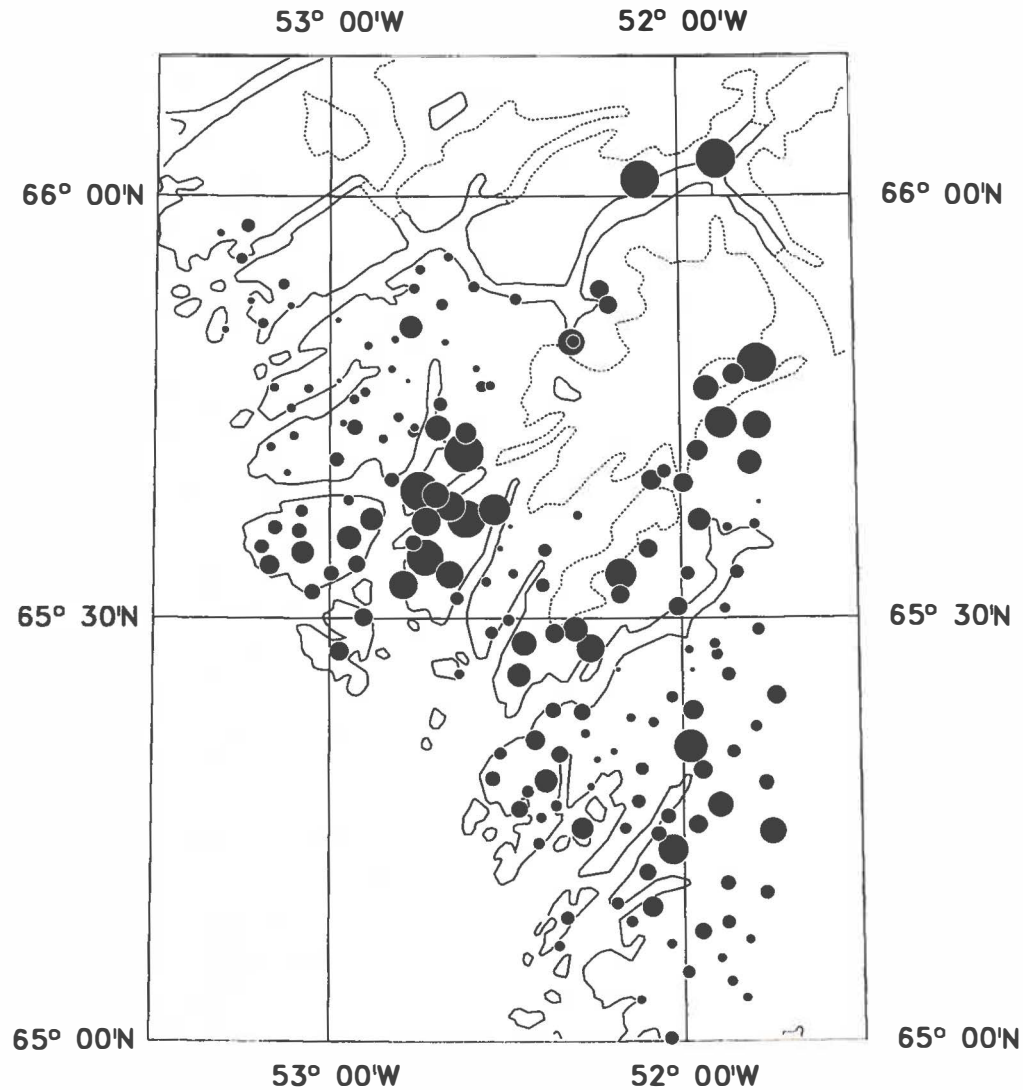
50 km





# Rb in stream sediment

Fig. 24



Rb ppm

X-ray Fluorescence

Number of samples:	173
Min. value:	2
Max. value:	104
Mean:	34
Median:	30
Variance:	308
Std. Dev.:	18

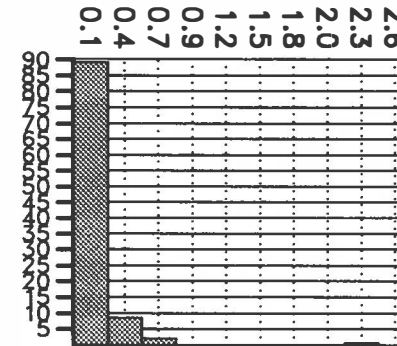
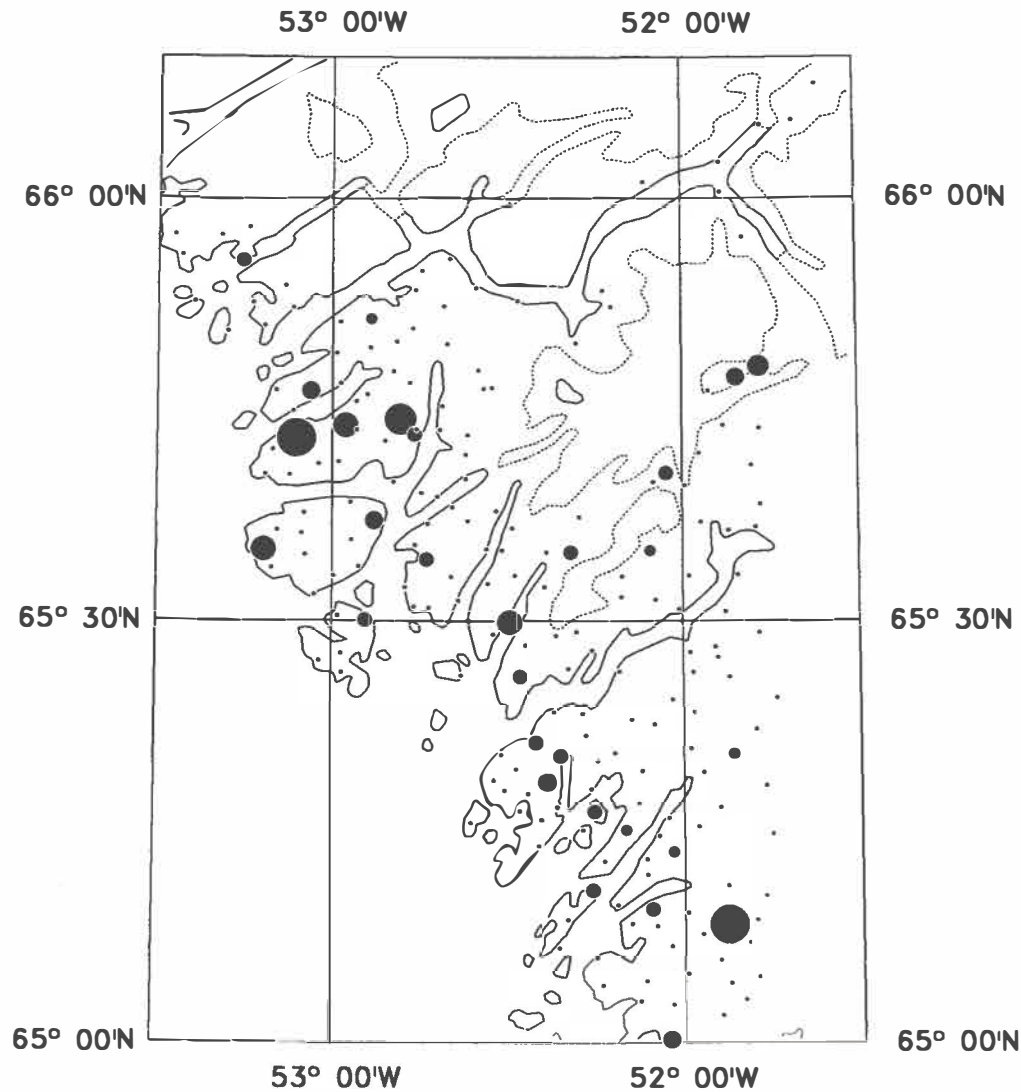
50 km





# Sb in stream sediment

Fig. 25



Sb ppm

INAA

Number of samples:	211
Min. value:	0.0
Max. value:	6.5
Mean:	0.1
Median:	0.0
Variance:	0.2
Std. Dev.:	0.5

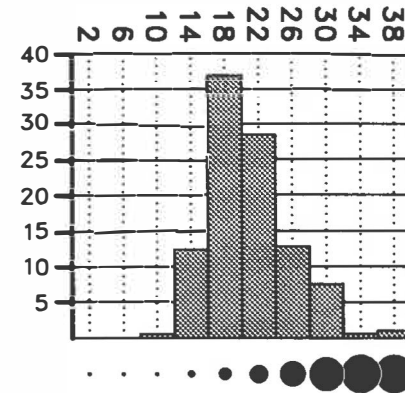
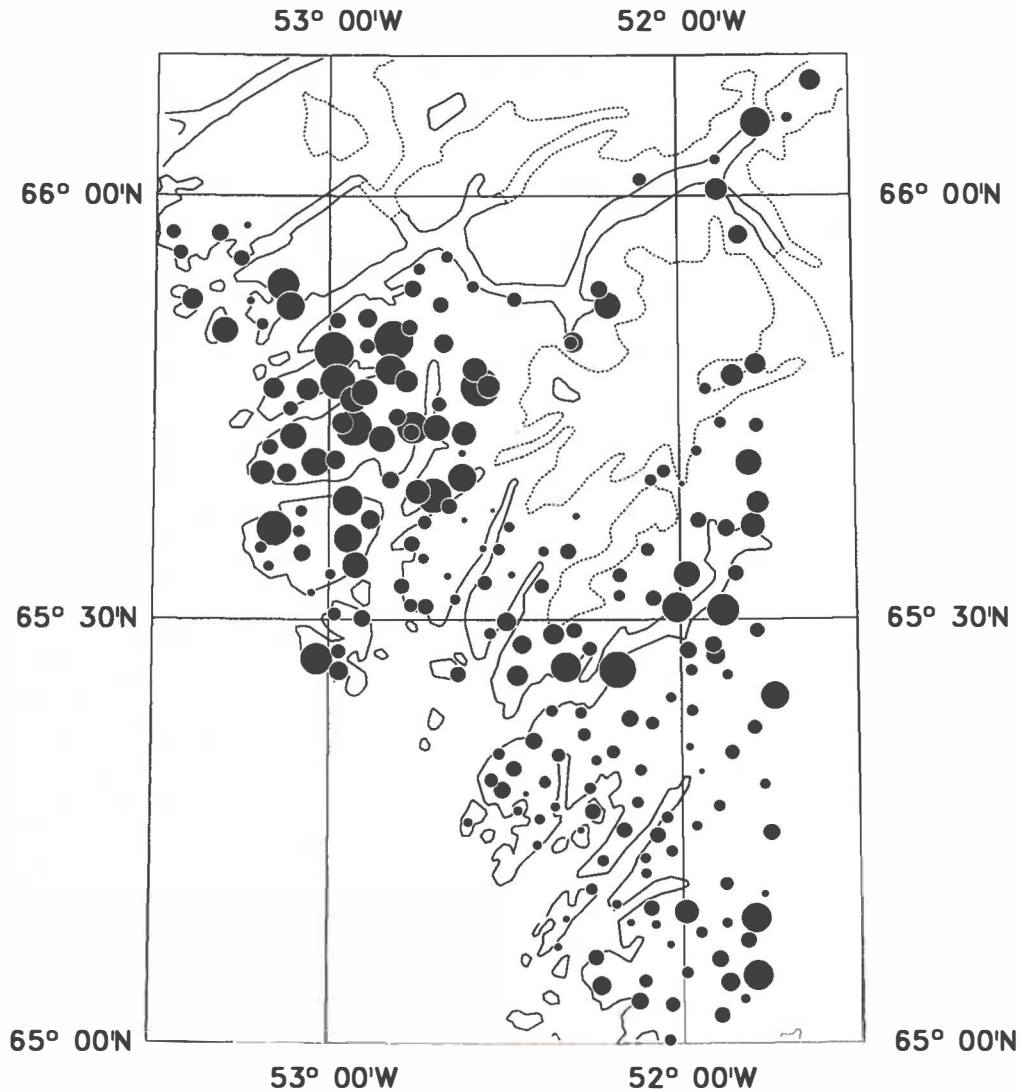
50 km





# Sc in stream sediment

Fig. 26



Sc ppm

INAA

Number of samples:	211
Min. value:	10
Max. value:	37
Mean:	20
Median:	19
Variance:	23
Std. Dev.:	5

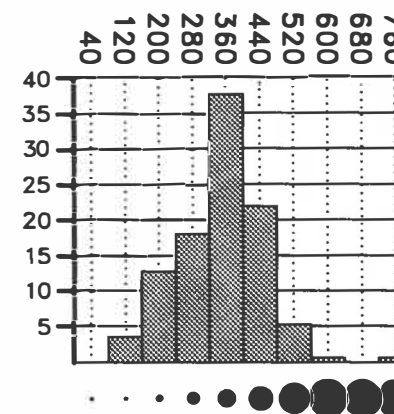
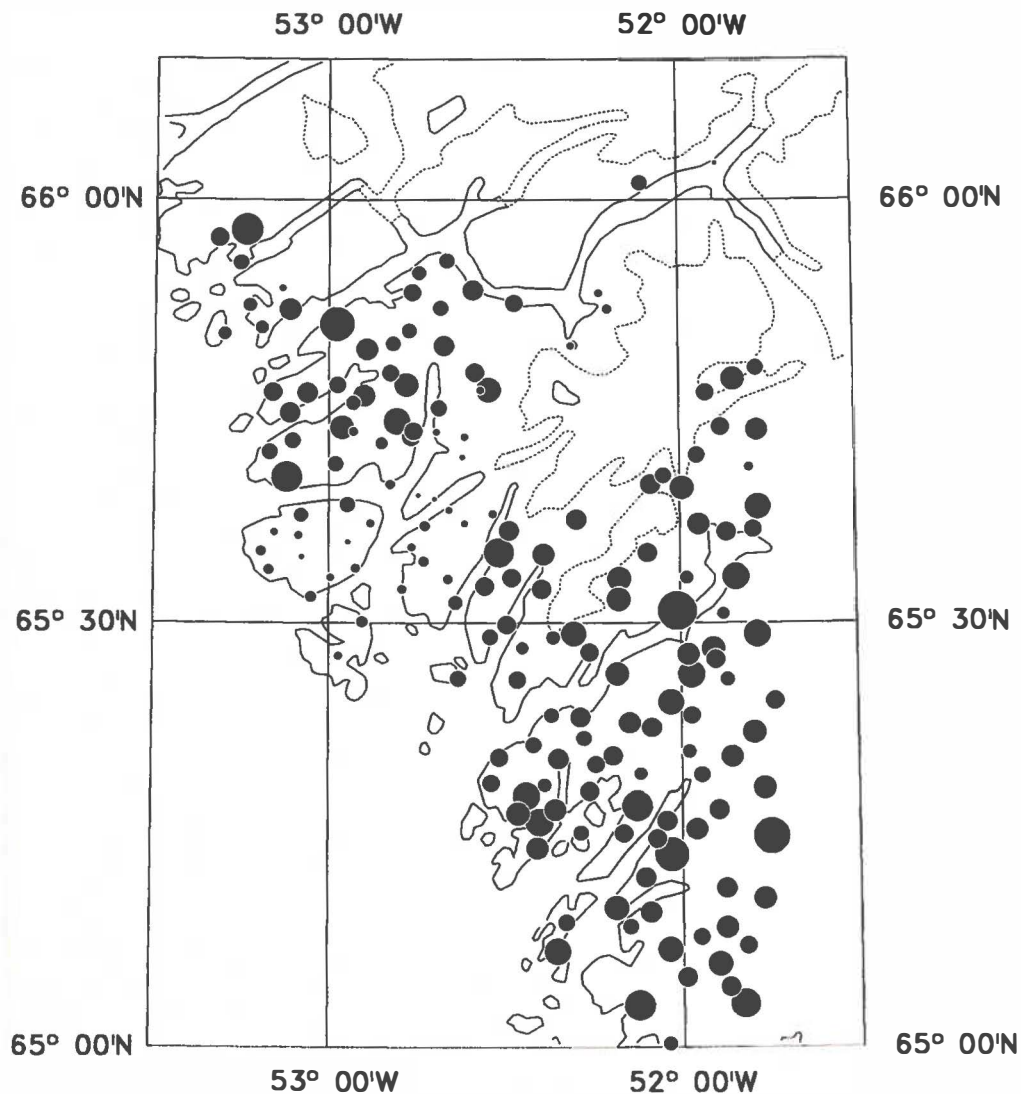
50 km





# Sr in stream sediment

Fig. 27



Sr ppm

X-ray Fluorescence

Number of samples:	173
Min. value:	132
Max. value:	762
Mean:	346
Median:	351
Variance:	9423
Std. Dev.:	97

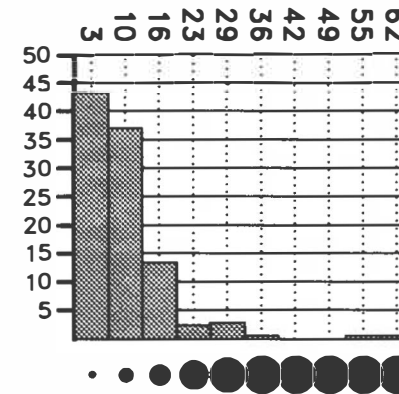
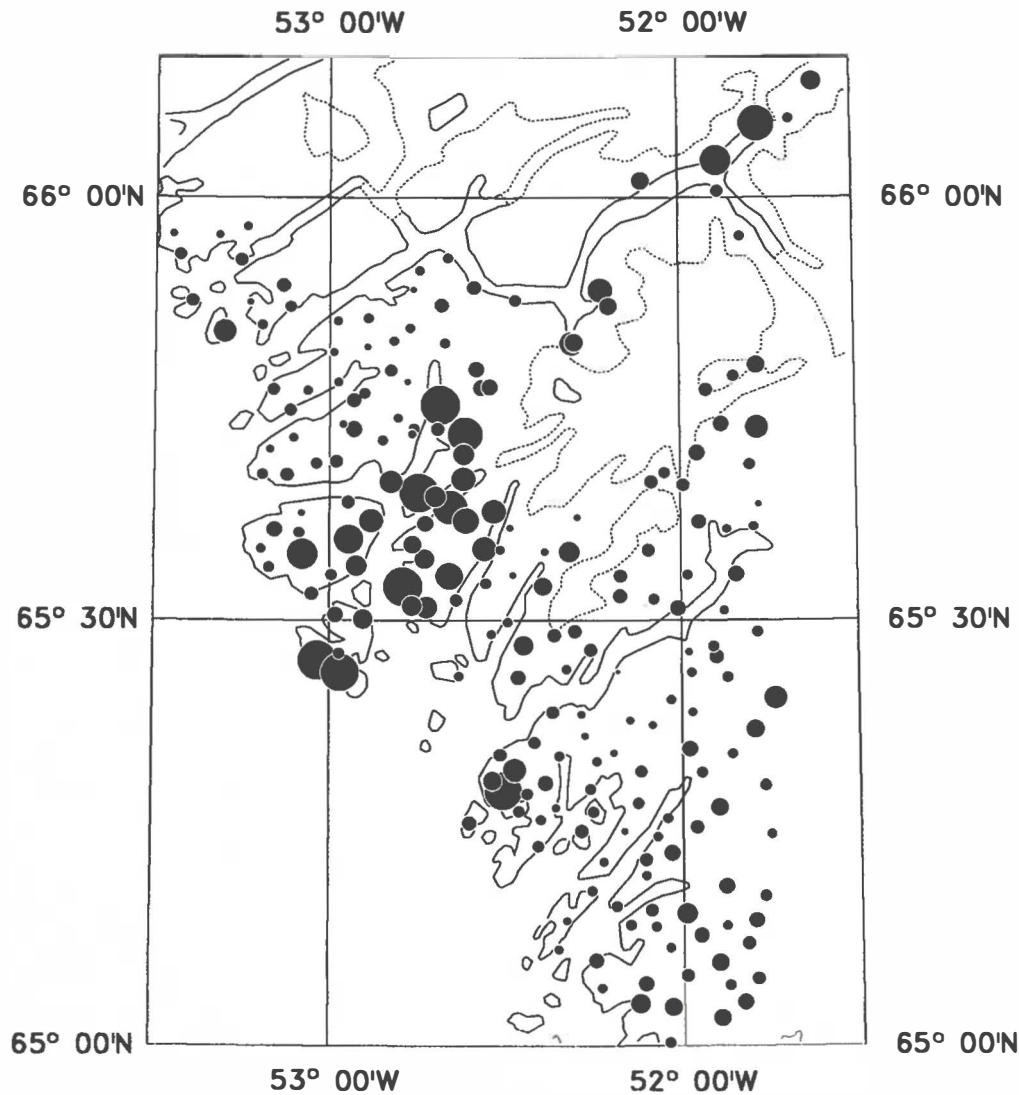
50 km





Th in stream sediment

Fig. 28



Th ppm  
INAA

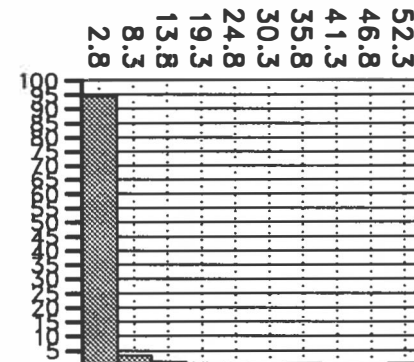
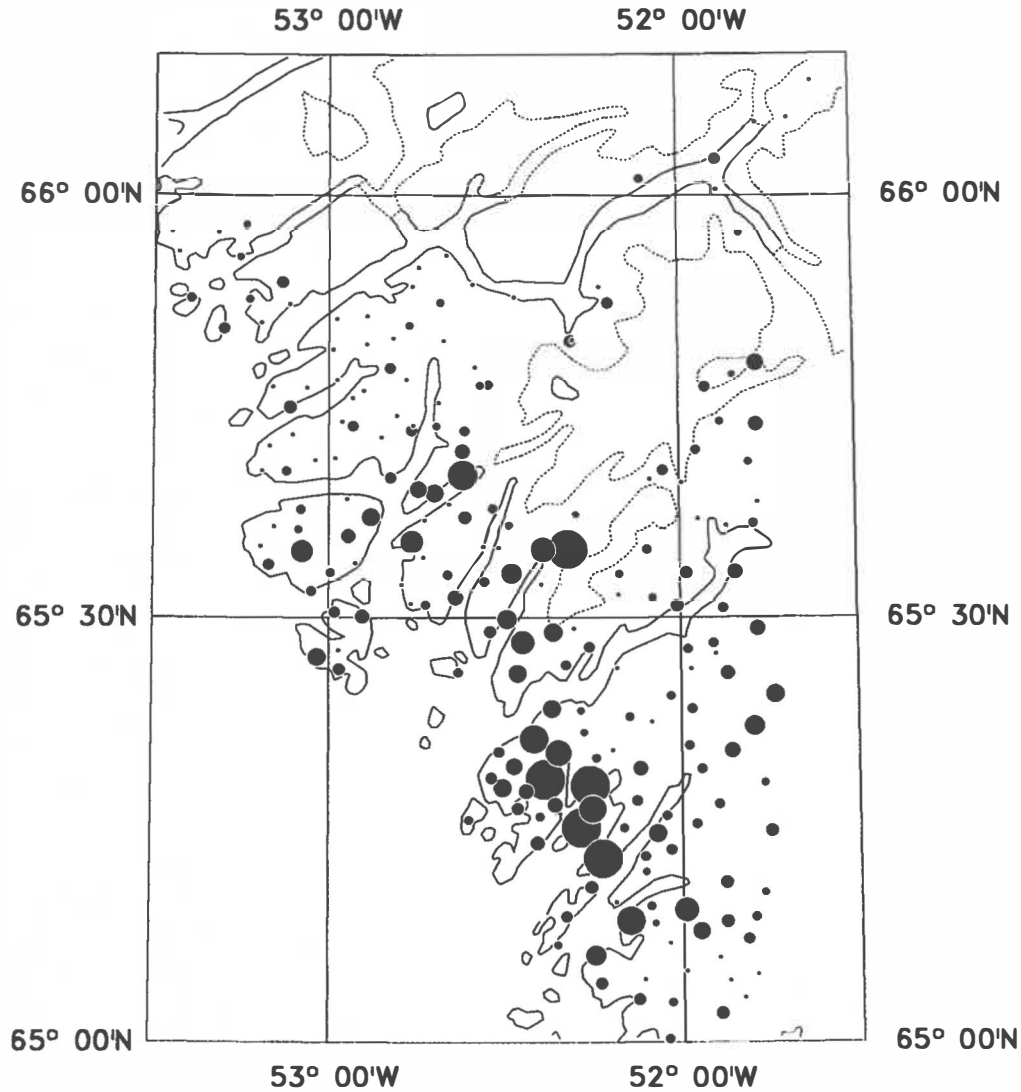
Number of samples:	211
Min. value:	0
Max. value:	61
Mean:	9
Median:	7
Variance:	60
Std. Dev.:	8

50 km



# U in stream sediment

Fig. 29



52.3  
46.8  
41.3  
35.8  
30.3  
24.8  
19.3  
13.8  
8.3  
2.8

U ppm

INAA

Number of samples:	211
Min. value:	0.0
Max. value:	54.0
Mean:	2.2
Median:	1.4
Variance:	22.9
Std. Dev.:	4.8

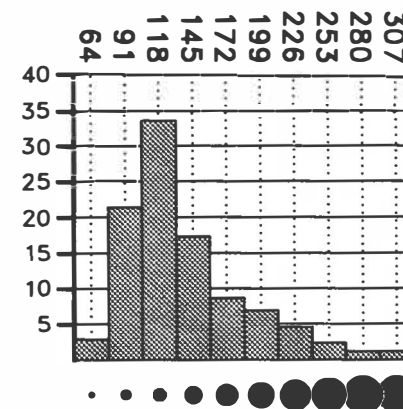
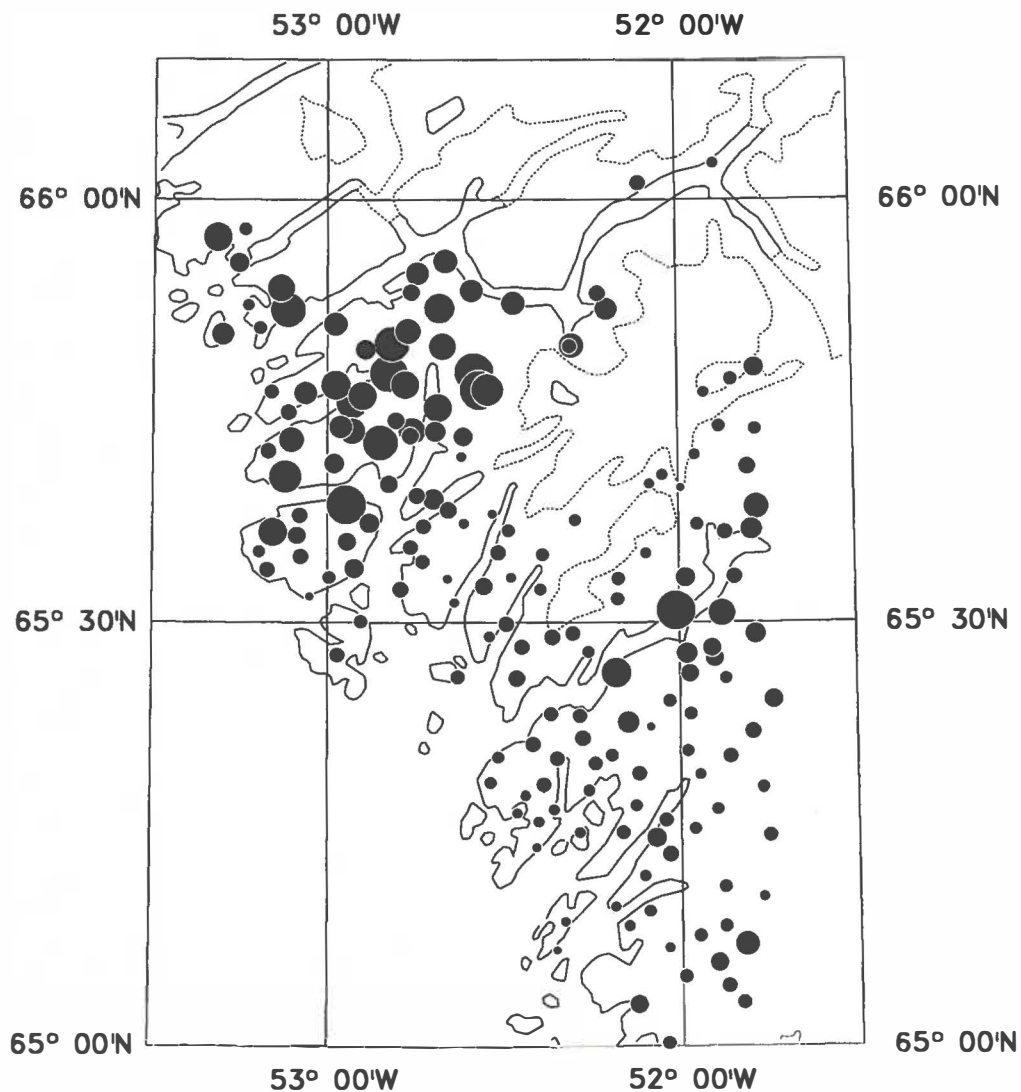
50 km





V in stream sediment

Fig. 30



V ppm

X-ray Fluorescence

Number of samples:	173
Min. value:	71
Max. value:	311
Mean:	137
Median:	124
Variance:	2297
Std. Dev.:	48

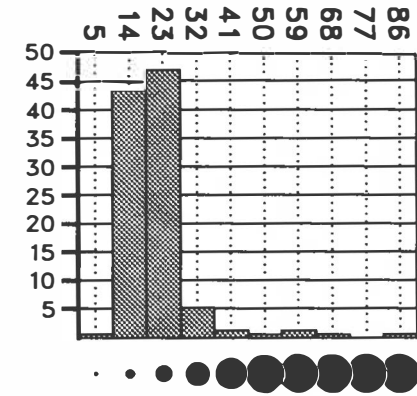
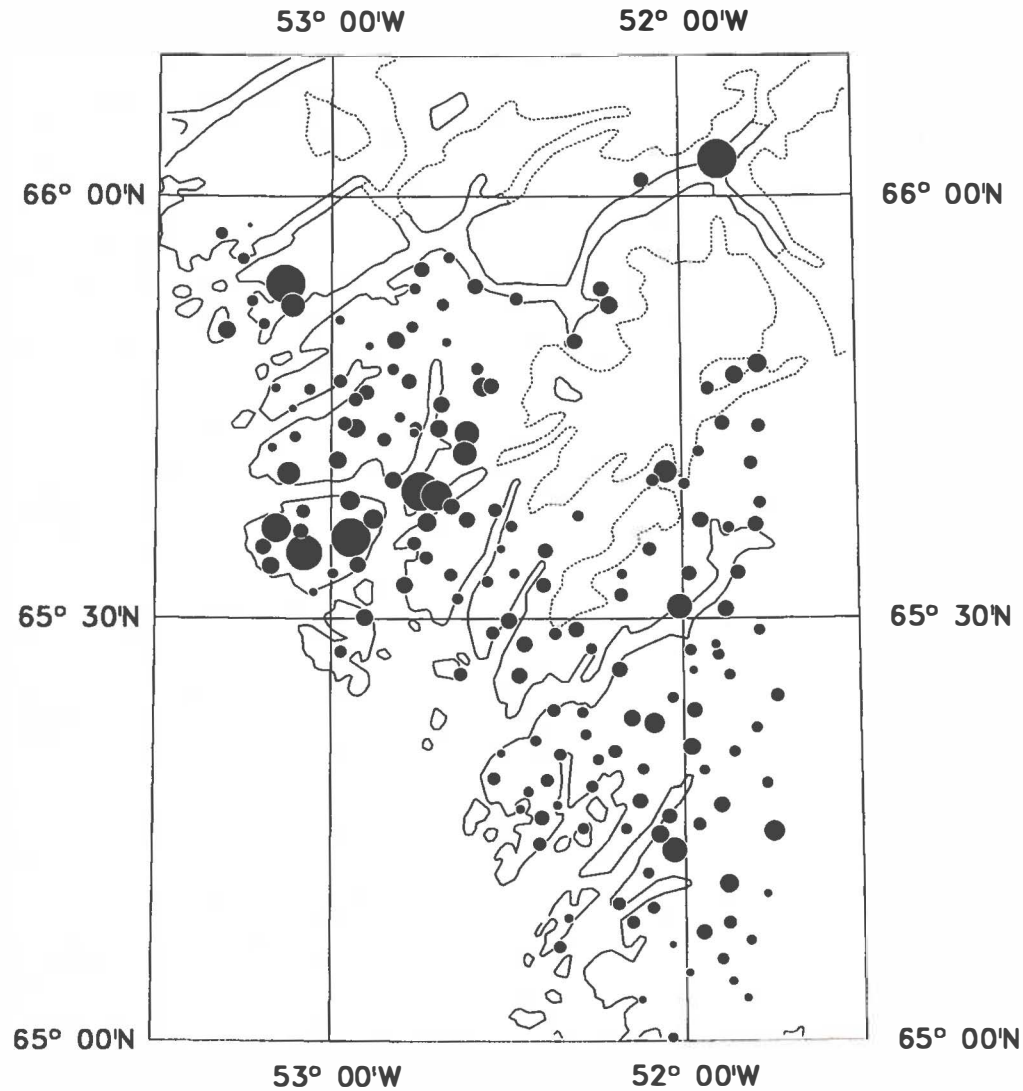
50 km





# Y in stream sediment

Fig. 31



Y ppm

X-ray Fluorescence

Number of samples:	173
Min. value:	7
Max. value:	88
Mean:	20
Median:	18
Variance:	87
Std. Dev.:	9

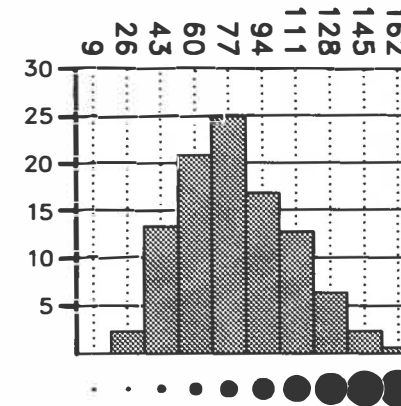
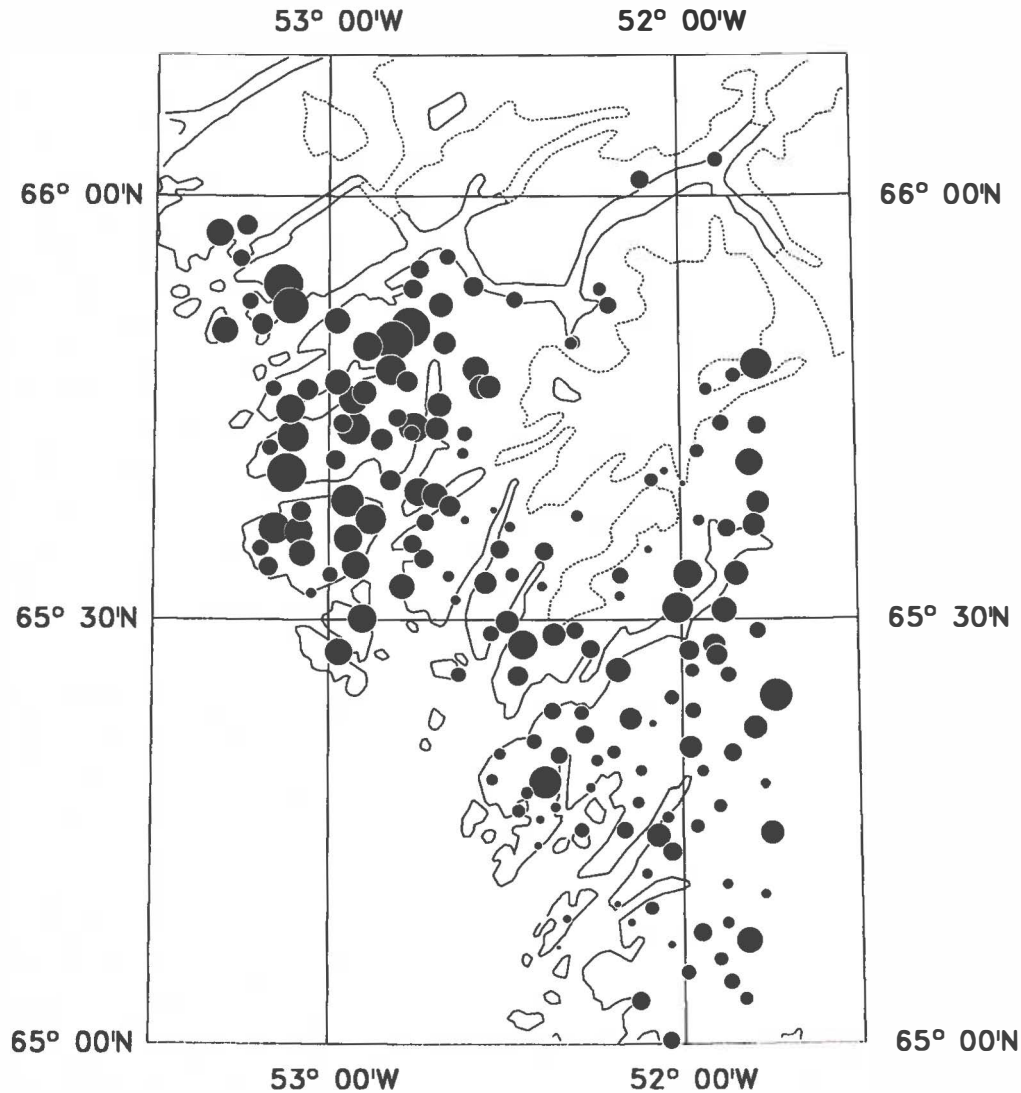
50 km





# Zn in stream sediment

Fig. 32



Zn ppm

X-ray Fluorescence

Number of samples:	173
Min. value:	22
Max. value:	165
Mean:	79
Median:	76
Variance:	772
Std. Dev.:	28

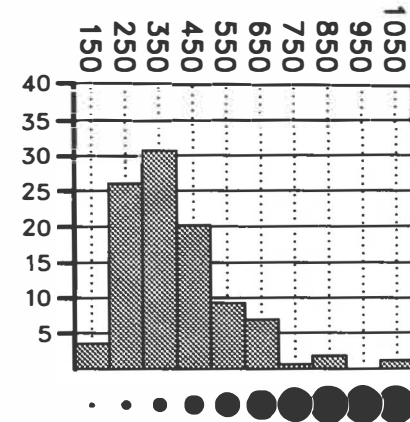
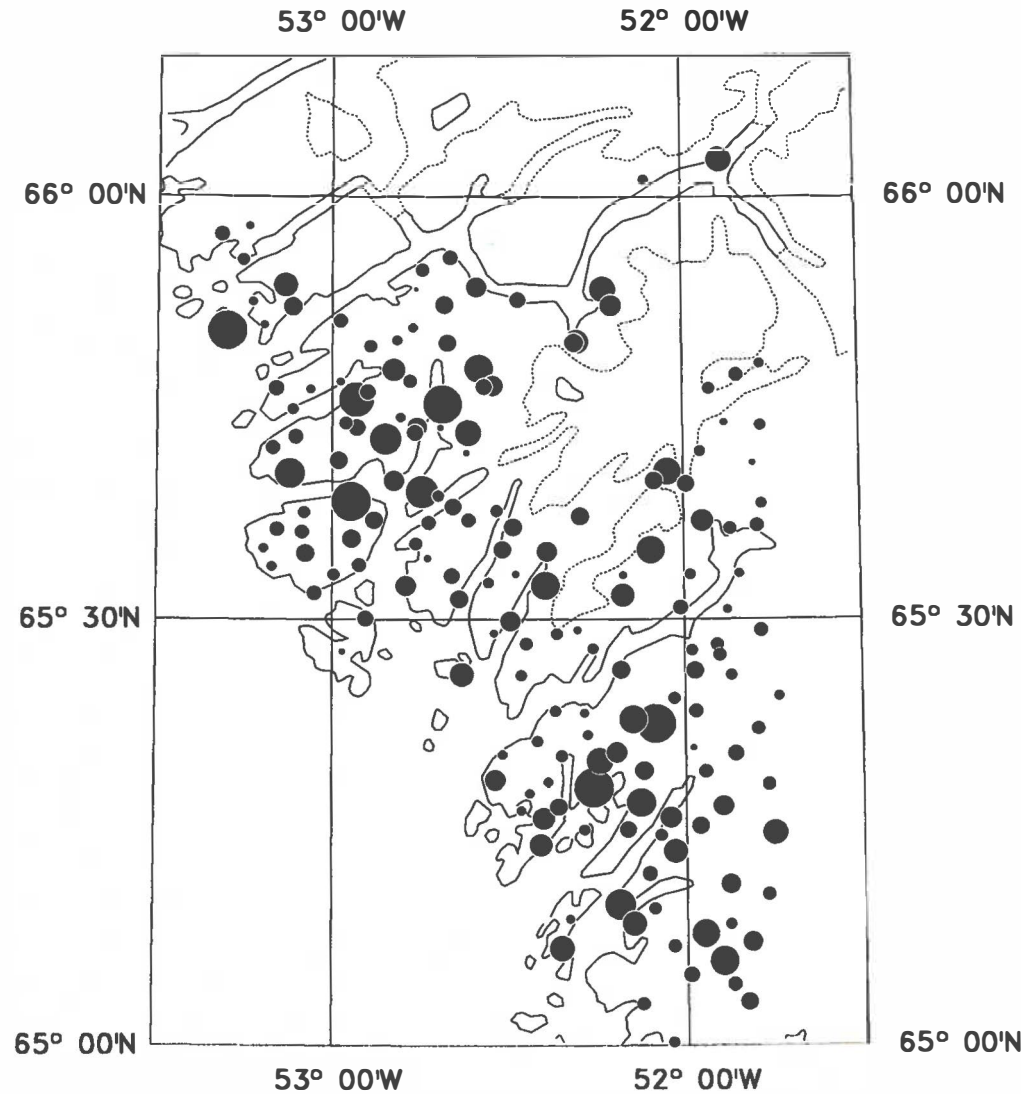
50 km





# Zr in stream sediment

Fig. 33



Zr ppm

X-ray Fluorescence

Number of samples:	173
Min. value:	110
Max. value:	1073
Mean:	392
Median:	352
Variance:	24793
Std. Dev.:	157

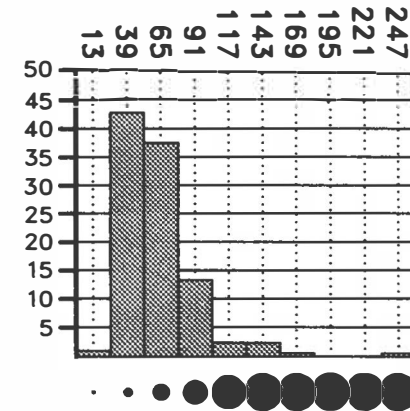
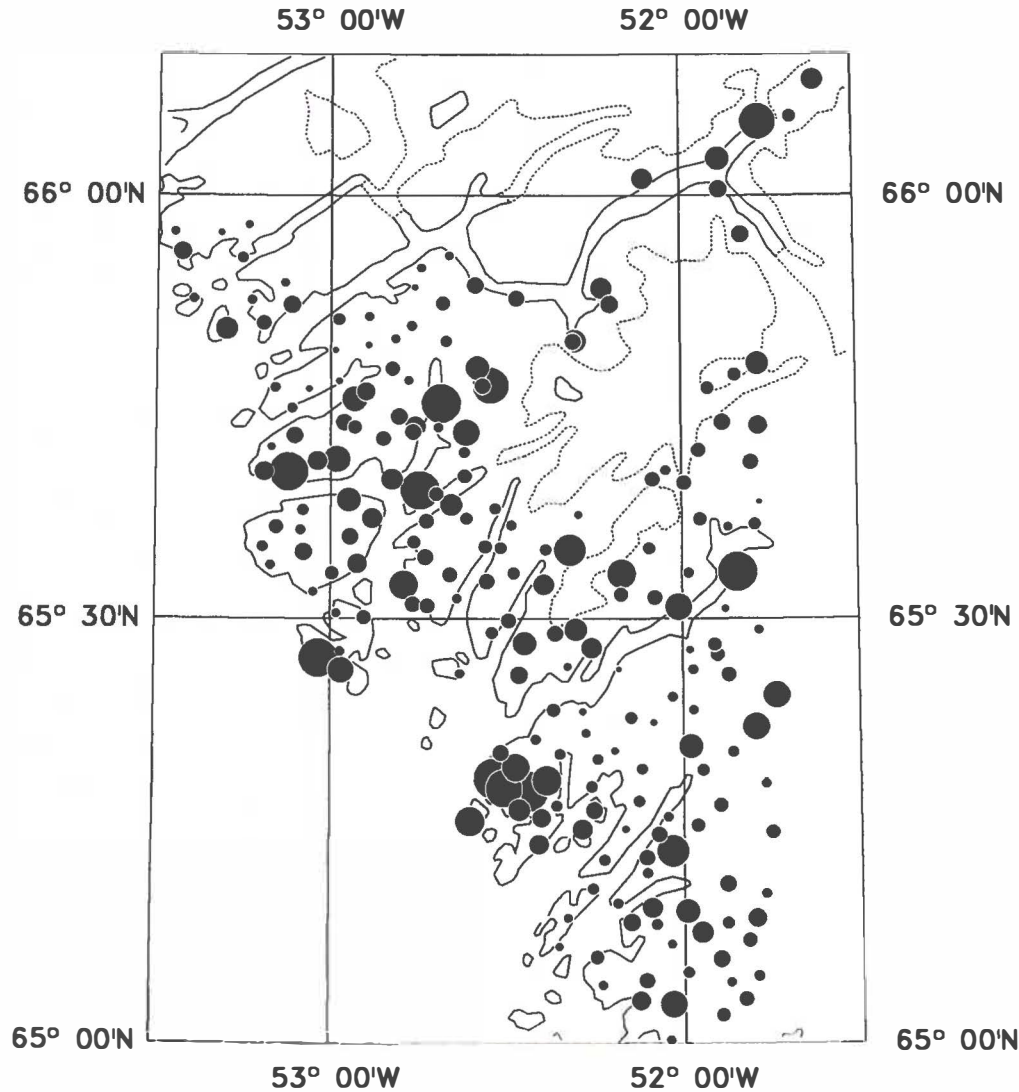
50 km





# La in stream sediment

Fig. 34



La ppm

INAA

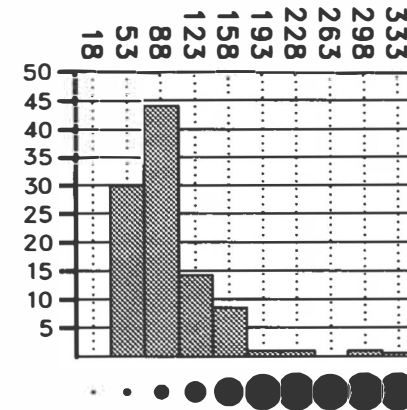
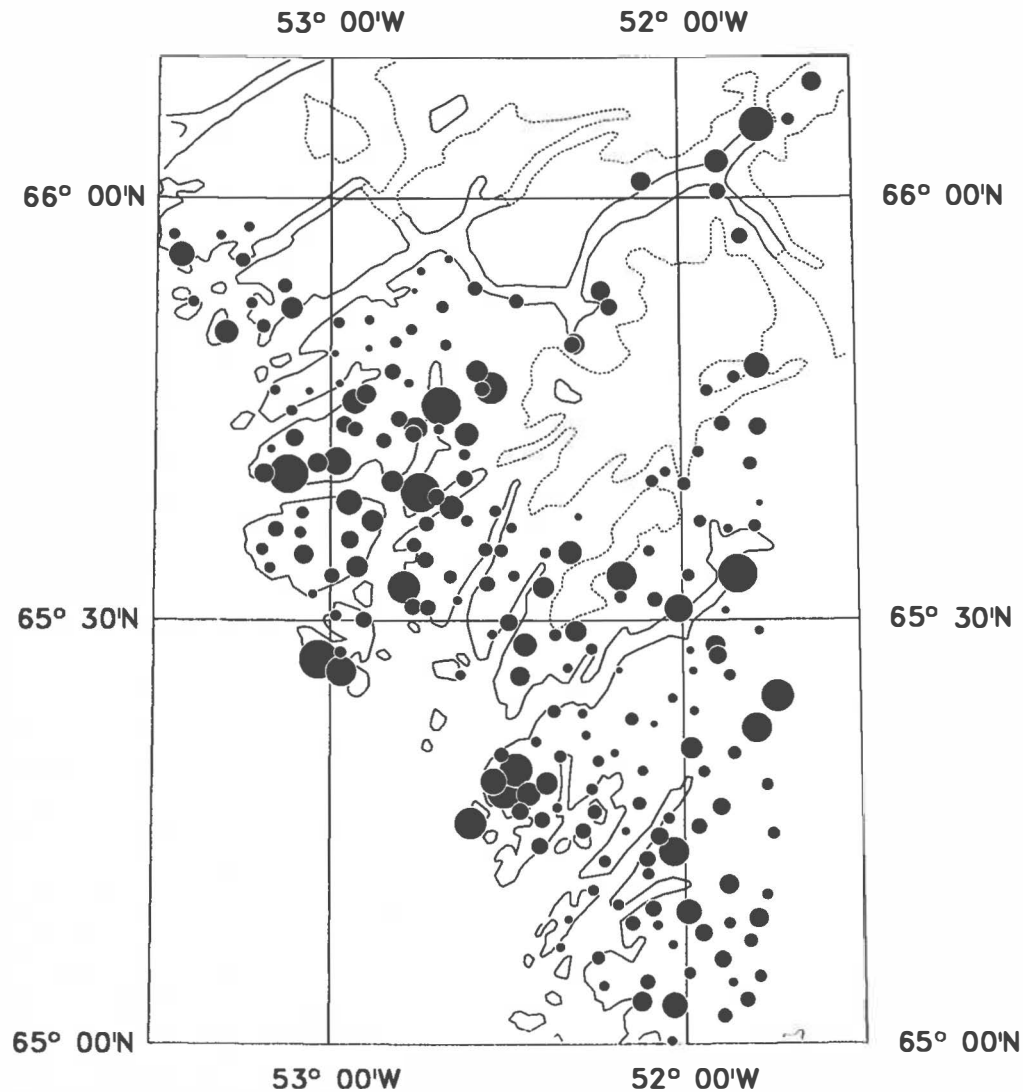
Number of samples:	211
Min. value:	24
Max. value:	250
Mean:	60
Median:	54
Variance:	780
Std. Dev.:	28

50 km



# Ce in stream sediment

Fig. 35



Ce ppm

INAA

Number of samples:	211
Min. value:	38
Max. value:	340
Mean:	93
Median:	81
Variance:	1804
Std. Dev.:	42

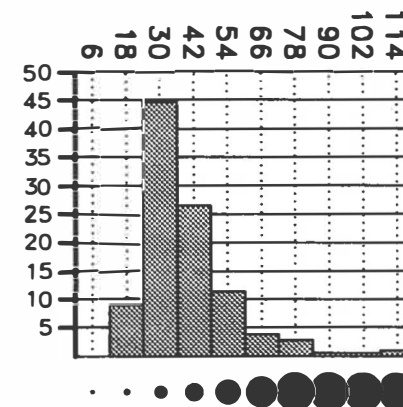
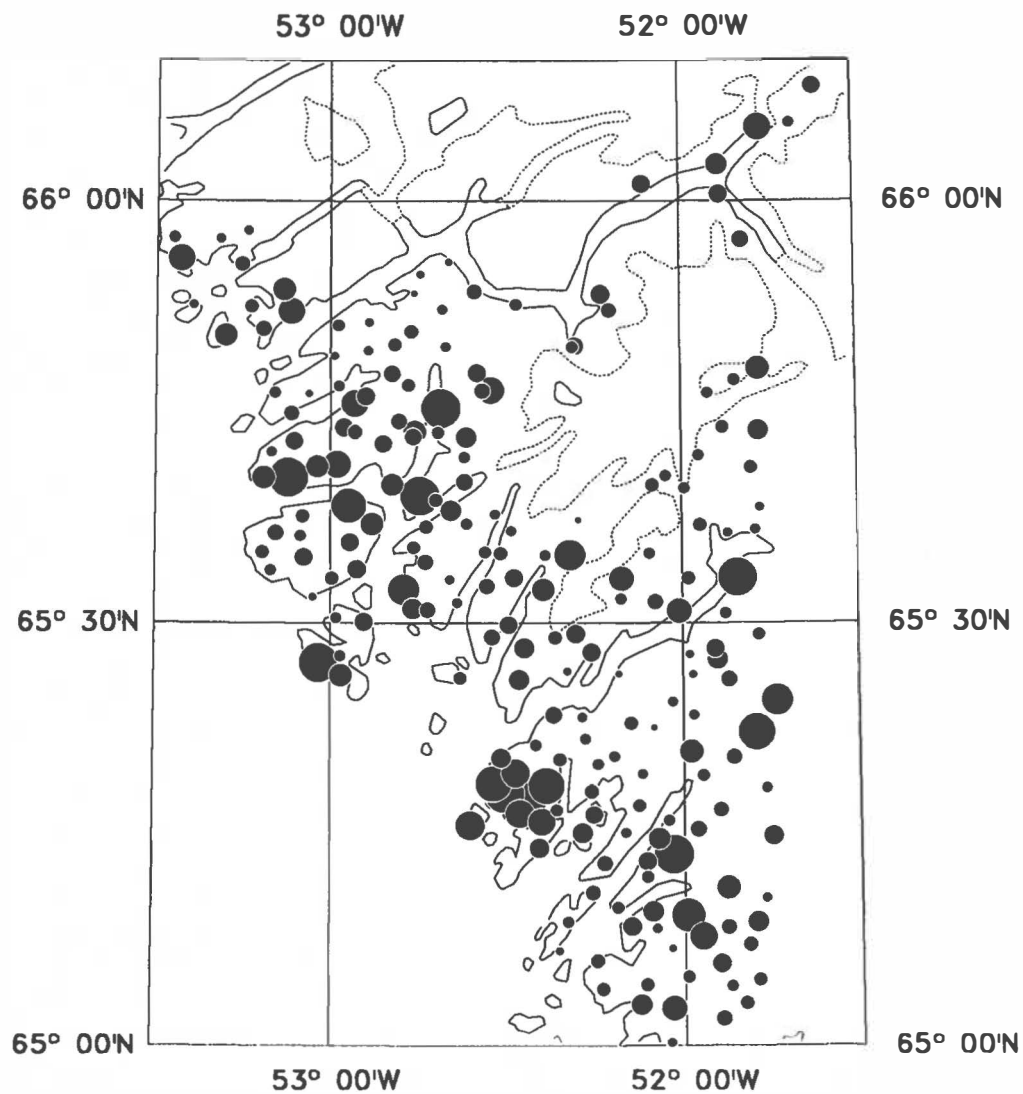
50 km





# Nd in stream sediment

Fig. 36



Nd ppm

INAA

Number of samples:	211
Min. value:	16
Max. value:	118
Mean:	38
Median:	34
Variance:	264
Std. Dev.:	16

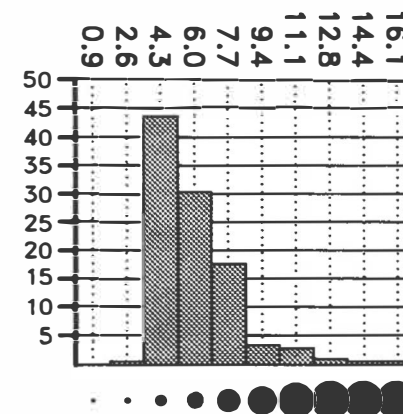
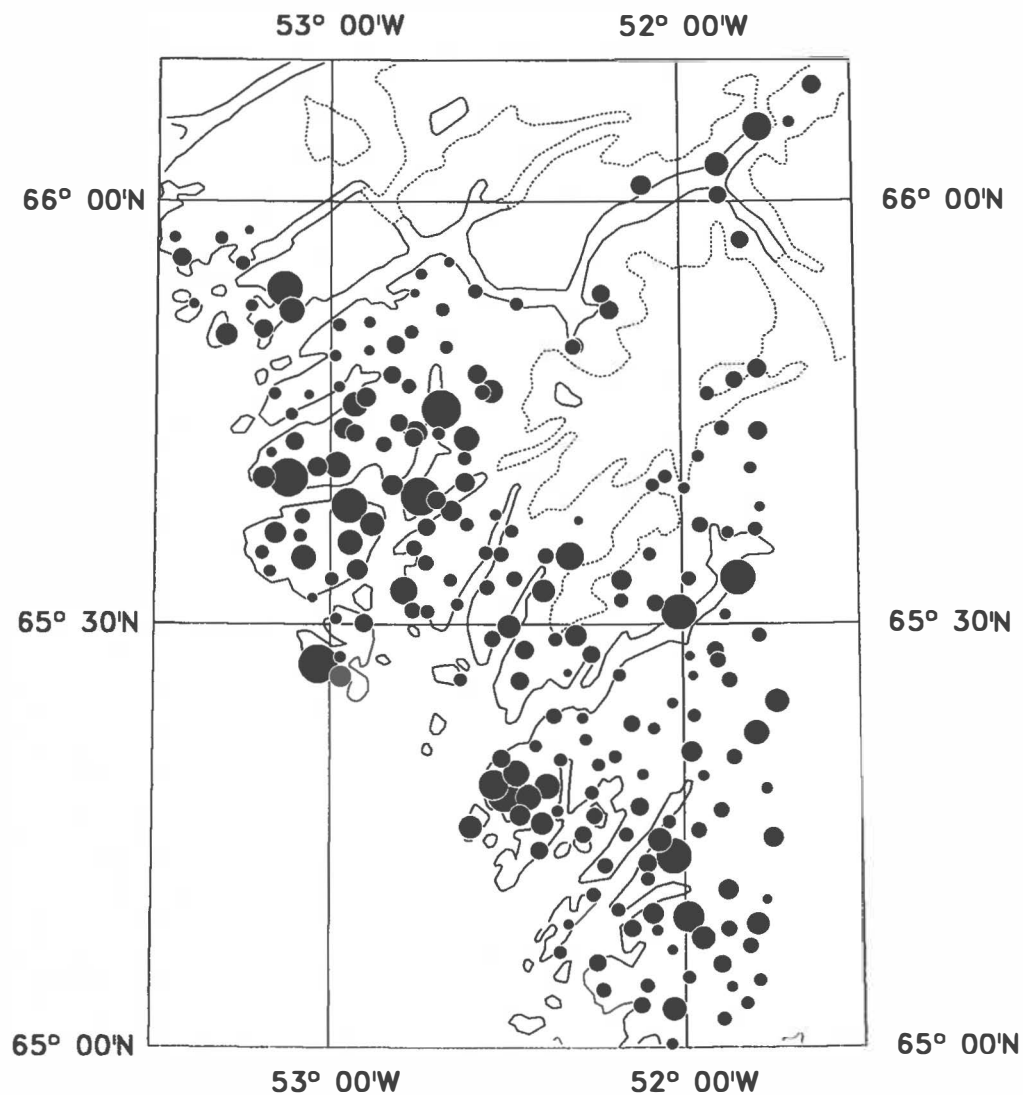
50 km





# Sm in stream sediment

Fig. 37



Sm ppm

INAA

Number of samples:	211
Min. value:	3.2
Max. value:	16.0
Mean:	6.0
Median:	5.4
Variance:	4.0
Std. Dev.:	2.0

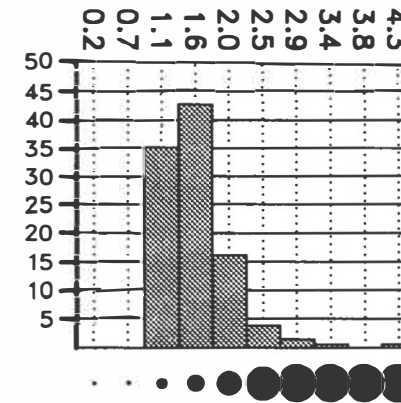
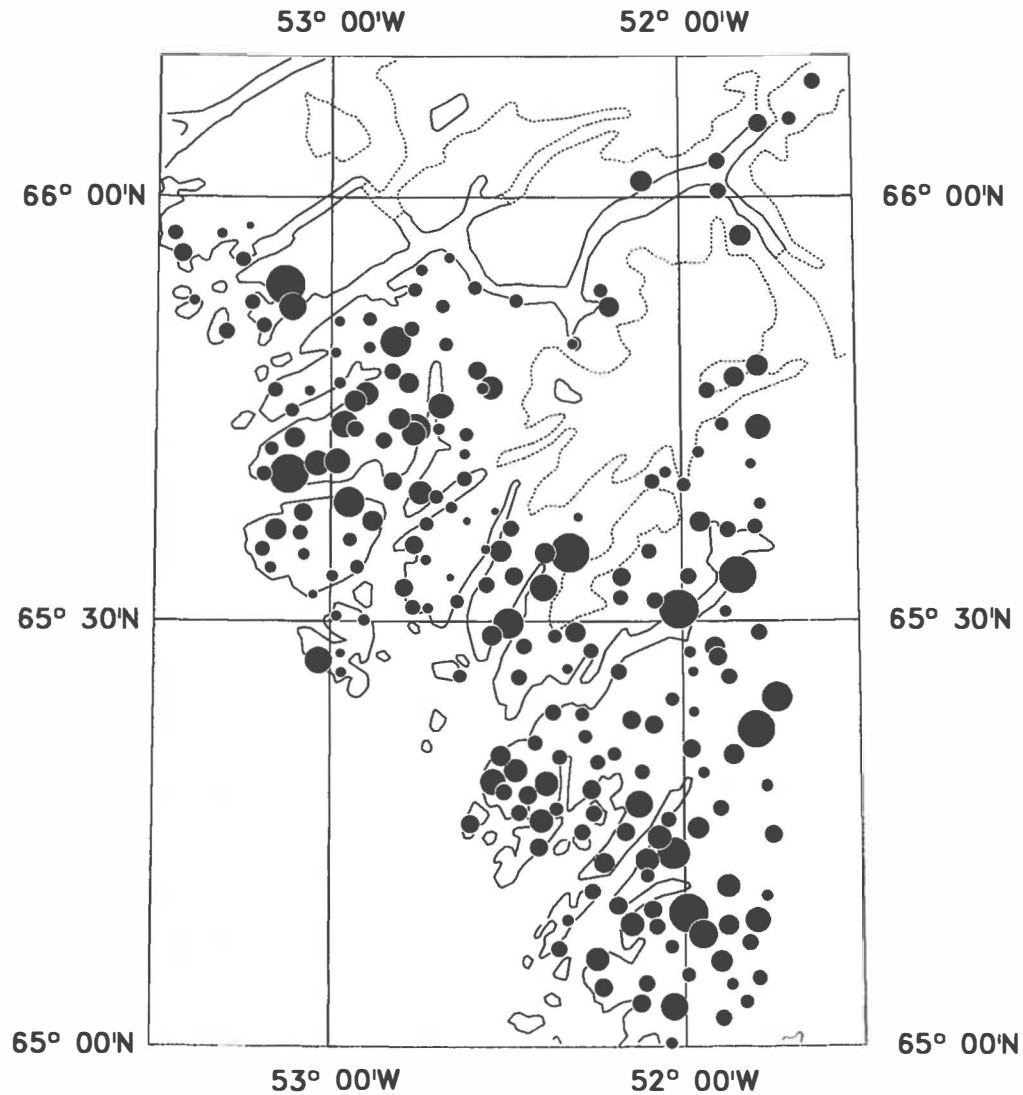
50 km





# Eu in stream sediment

Fig. 38



Eu ppm  
INAA

Number of samples:	211
Min. value:	0.9
Max. value:	4.3
Mean:	1.6
Median:	1.5
Variance:	0.2
Std. Dev.:	0.4

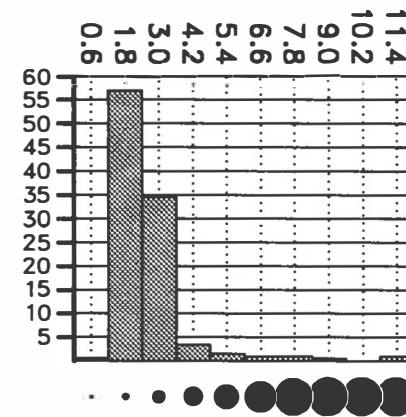
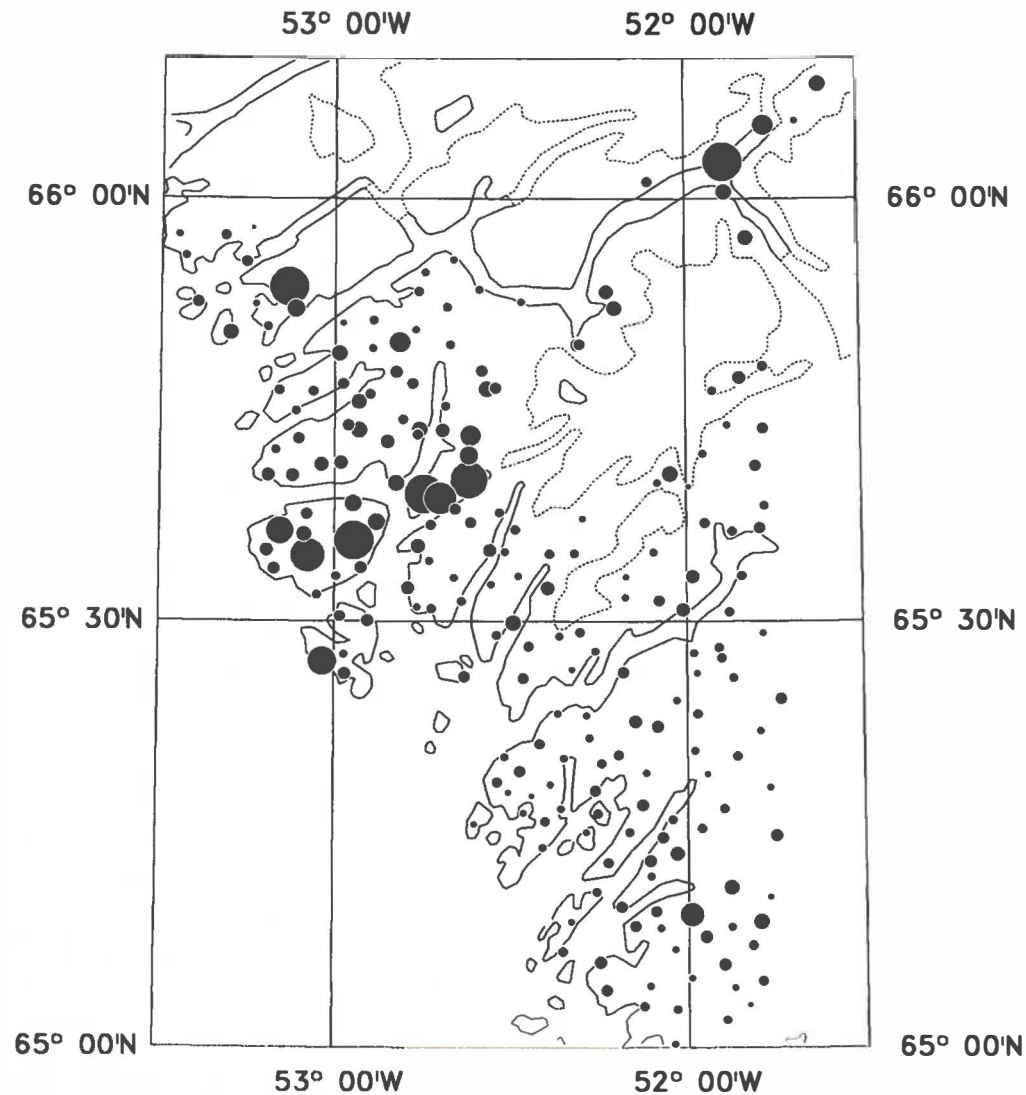
50 km





# Yb in stream sediment

Fig. 39



Yb ppm  
INAA

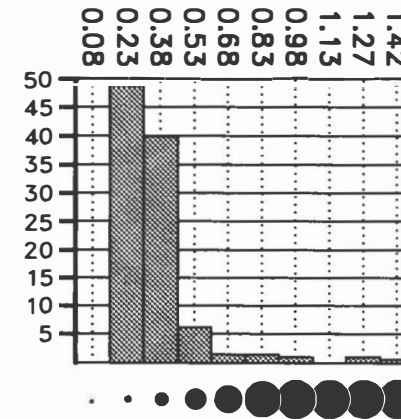
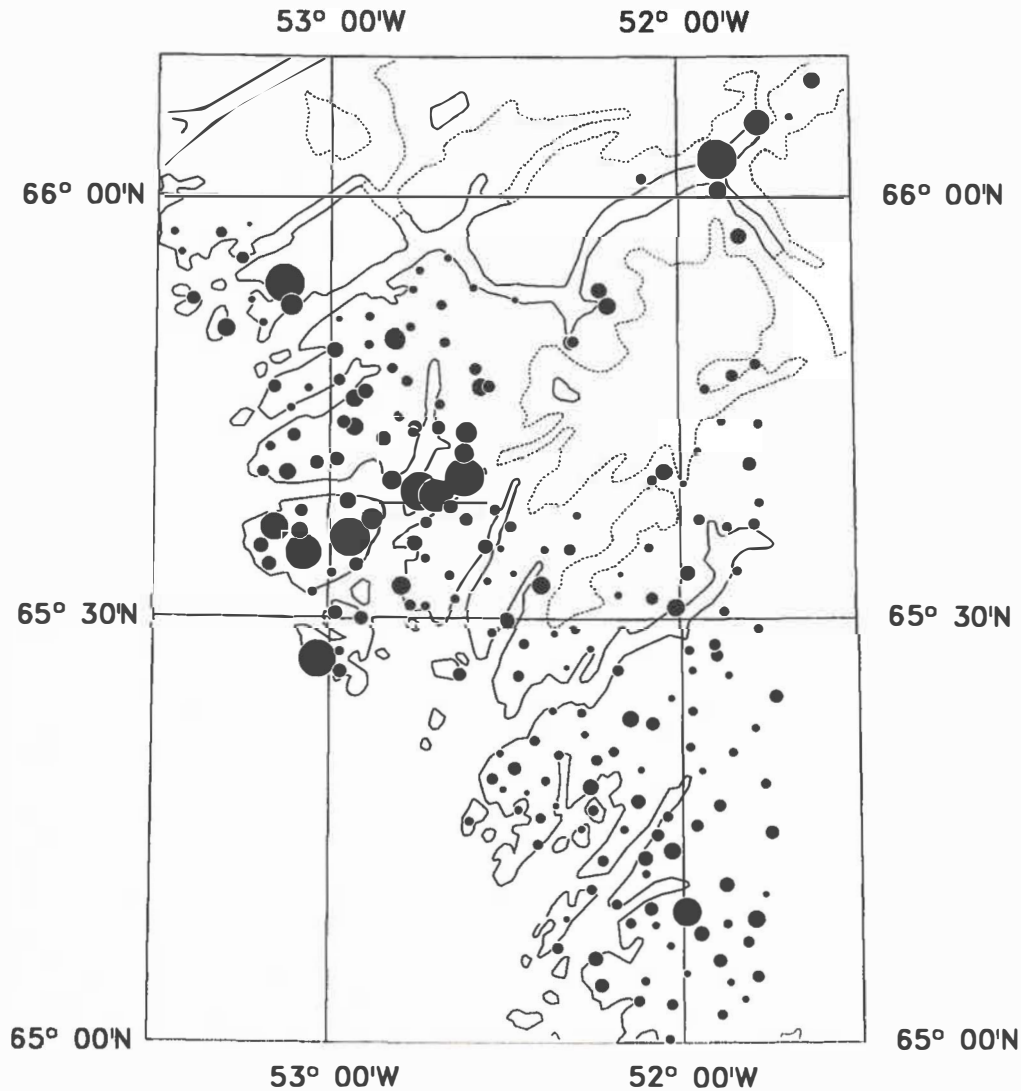
Number of samples:	211
Min. value:	1.0
Max. value:	11.0
Mean:	2.6
Median:	2.2
Variance:	1.9
Std. Dev.:	1.4





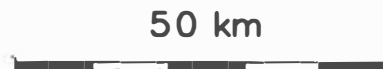
# Lu in stream sediment

Fig. 40



Lu ppm  
INAA

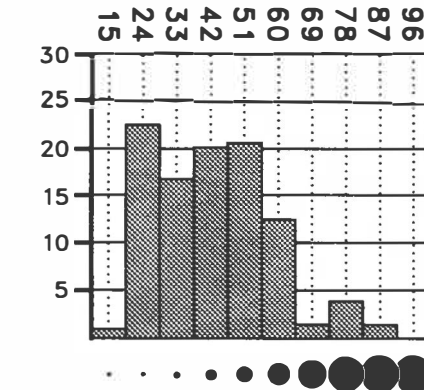
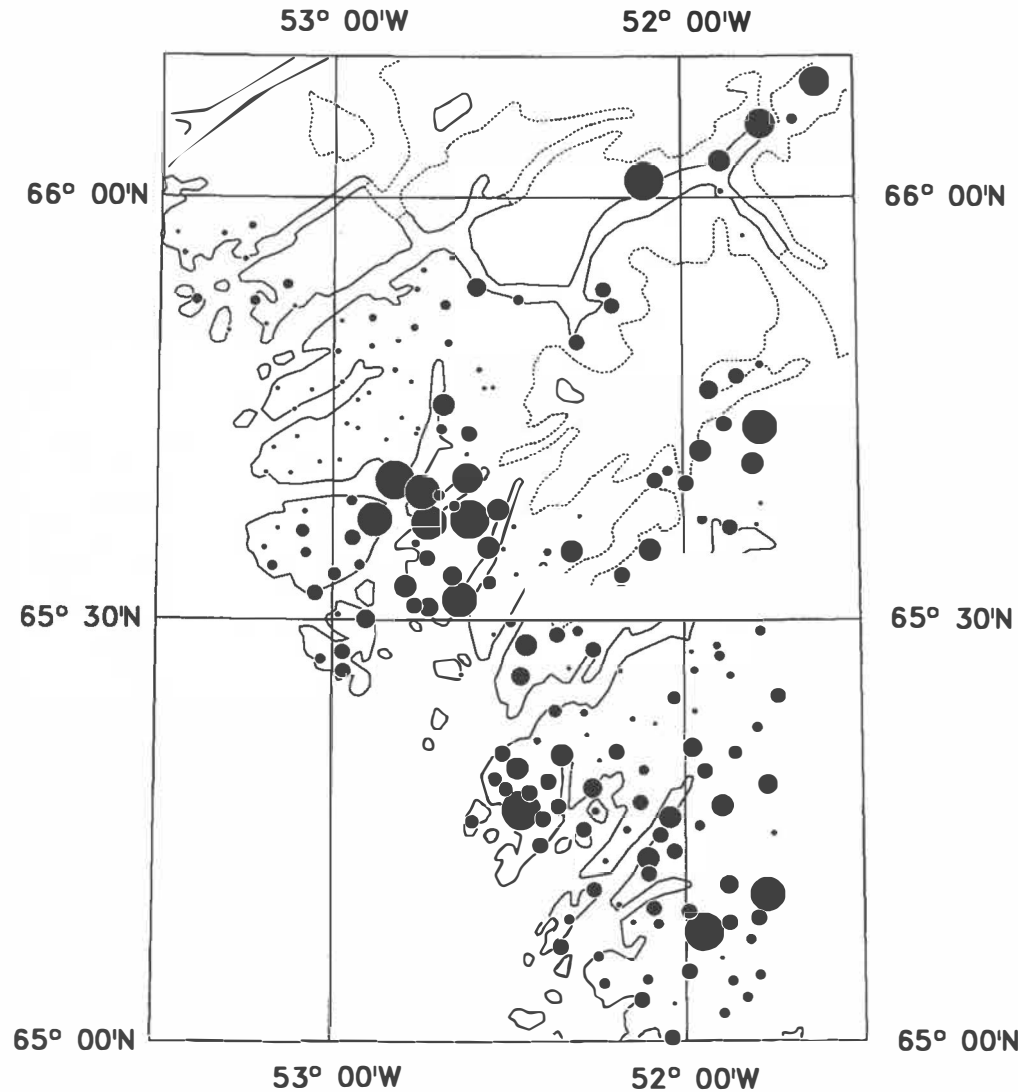
Number of samples:	211
Min. value:	0.16
Max. value:	1.42
Mean:	0.34
Median:	0.30
Variance:	0.03
Std. Dev.:	0.17





Total radiation

Fig. 41



Counts per sec.

Scintillometry

Number of samples:	210
Min. value:	15
Max. value:	100
Mean:	42
Median:	40
Variance:	244
Std. Dev.:	16

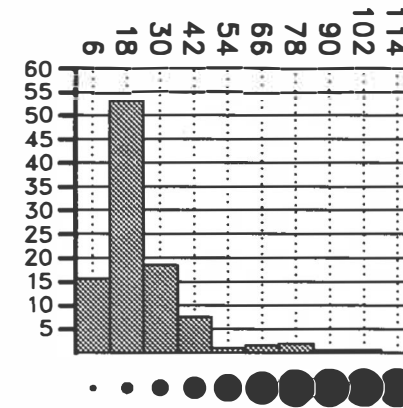
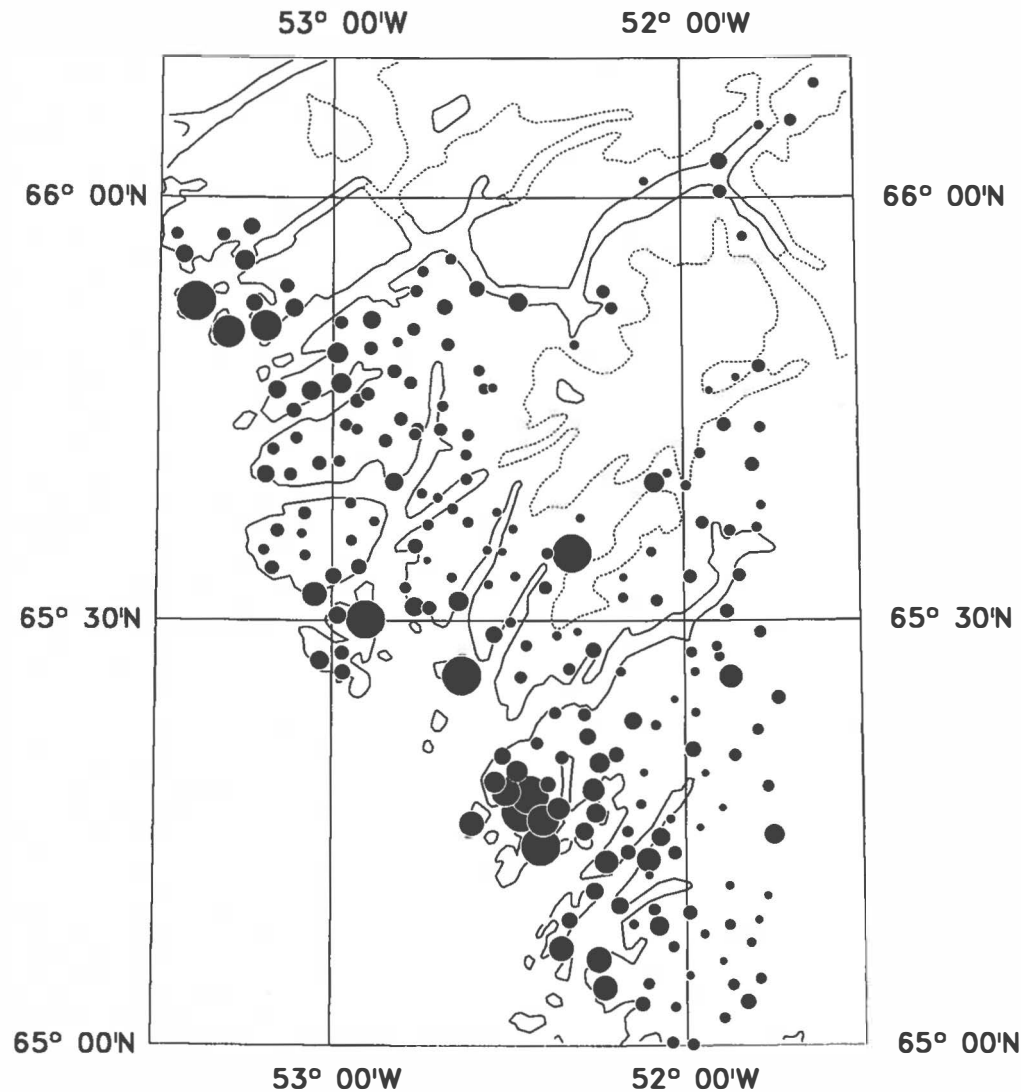
50 km





# Conductivity of stream water

Fig. 42



Micro Sievert

Number of samples:	212
Min. value:	7
Max. value:	258
Mean:	24
Median:	19
Variance:	492
Std. Dev.:	22

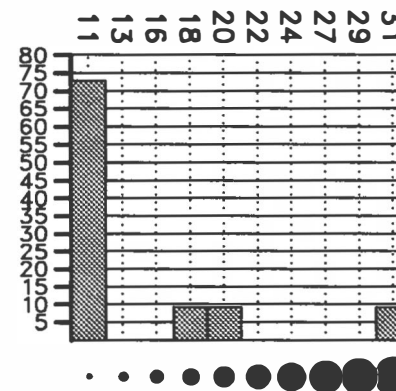
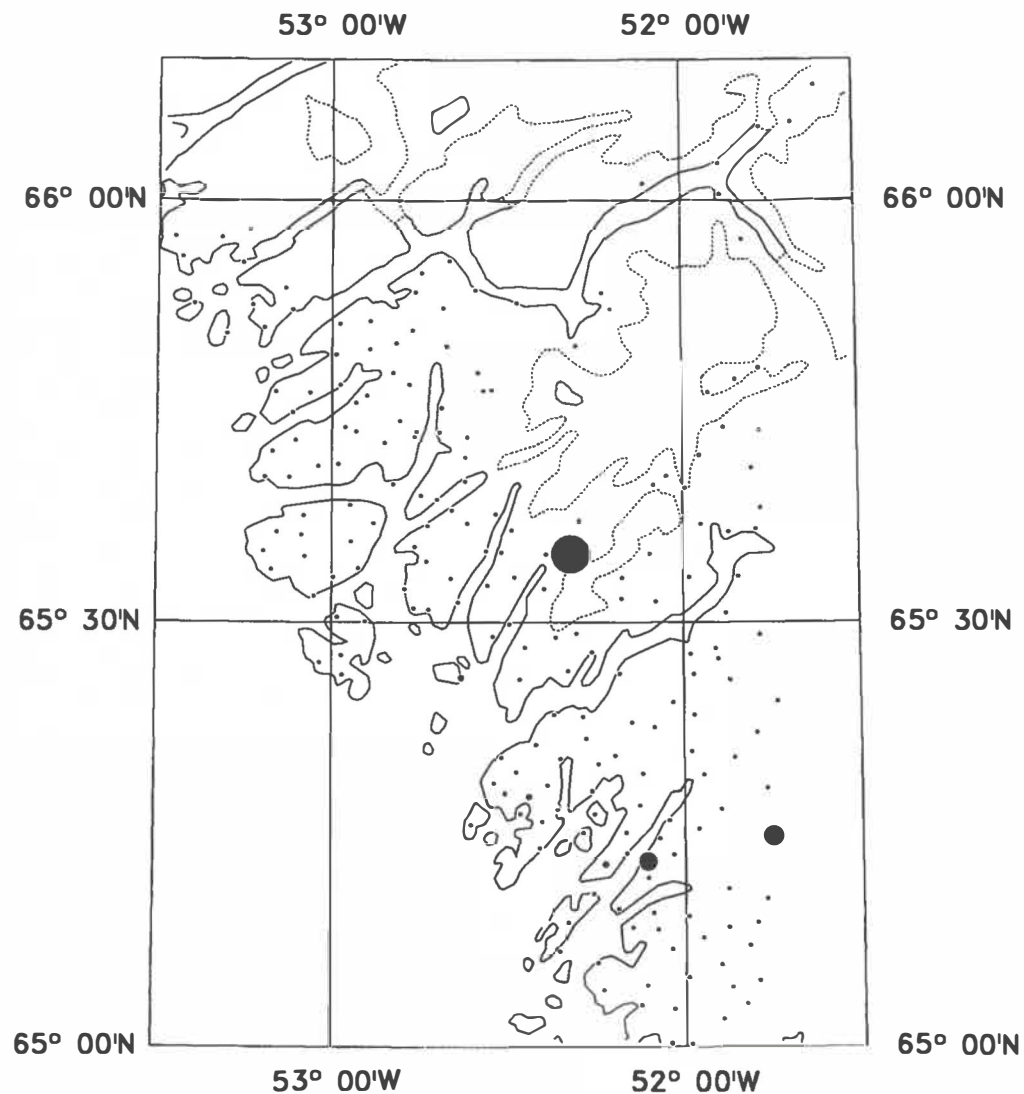
50 km





# F in stream water

Fig. 43



F ppb

Ion sensitive electrode

Number of samples:	212
Min. value:	0
Max. value:	31
Mean:	1
Median:	0
Variance:	11
Std. Dev.:	3

50 km





# Stream sediment anomalies

Fig. 44

